

Title of thesis

**A Novel Code Construction Technique and Detection Scheme
for the Double Weight Code Family for SAC OCDMA**

I, AHMED MOHAMMED ALHASSAN ALI

Here by allow my thesis to be placed at the Information Resource Center (IRC) of Universiti Teknologi PETRONAS (UTP) with the following conditions:

1. The thesis becomes the property of UTP.
2. The IRC of UTP may make copies of the thesis for academic purposes only.
3. This thesis is classified as

☐

Confidential

☒

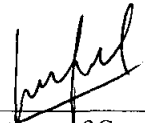
Non-confidential

If this thesis is confidential, please state the reason:

The contents of the thesis will remain confidential for _____ years.

Remarks on disclosure:

Endorsed by



Signature of Author

Signature of Supervisor

Permanent: *Faculty of Electronics Engineering*
Address *Neelain University*
 Khartoum, Sudan

Name of Supervisor
Dr. Mohamad Naufal Mohamad Saad

Date: _____

Date: _____

UNIVERSITI TEKNOLOGI PETRONAS

Approval by Supervisor

The undersigned certify that they have read, and recommend to The Postgraduate Studies

Programme for acceptance, a thesis entitled

A Novel Code Construction Technique and Detection Scheme for the Double Weight

Code Family for SAC OCDMA

submitted by

Ahmed Mohammed Alhassan Ali

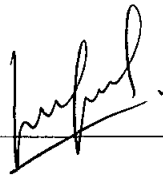
for the fulfilment of the requirements for the degree of

Masters of Science in Electrical and Electronics Engineering

Date

Signature

:



Main Supervisor

:

Dr. Mohamad Naufal bin Mohamad Saad

Date

:

Co-Supervisor

:

UNIVERSITI TEKNOLOGI PETRONAS

**A Novel Code Construction Technique and Detection Scheme for the Double
Weight Code Family for SAC OCDMA**

By

Ahmed Mohammed Alhassan Ali

A THESIS

SUBMITTED TO THE POSTGRADUATE STUDIES PROGRAMME

AS A REQUIREMENT FOR THE

DEGREE OF MASTERS OF SCIENCE IN ELECTRICAL AND ELECTRONICS

ENGINEERING

Electrical and Electronics Engineering

BANDAR SERI ISKANDAR,

PERAK

September, 2007

DECLARATION

I hereby declare that the thesis is based on my original work except for quotations and citations which have been duly acknowledged. I also declare that it has not been previously or concurrently submitted for any other degree at UTP or other institutions.

Signature: _____

Name : Ahmed Mohammed Alhassan Ali

Date : 21/09/2007

ACKNOWLEDGEMENT

- ✦ To my parents and family for their love, support and encouragement.
- ✦ To my supervisor Dr. Mohamad Naufal bin Mohamad Saad for his support and guidance that helped accomplish this work.
- ✦ To Dr. Syed Aljunid for his valuable time and advice.
- ✦ To the Electrical and Electronics Engineering Department, especially Mr. Azizuddin for his help and support.
- ✦ To all members of the Post Graduate Studies Office for help and advice.
- ✦ To all my friends and colleagues for the joy they brought into my life.

ABSTRACT

Spectral Amplitude Coding Optical Code Division Multiple Access (SAC OCDMA) systems are gaining more attention, due to the fact that when using appropriate detection technique, the Multiple Access Interference (MAI) can totally be canceled. There have been many codes proposed for SAC Optical CDMA systems, such as Hadamard code, Modified Frequency Hopping (MFH) code and Double Weight (DW) code family.

The motivation of this research is to enhance the DW code family to give an overall better performance. Three aspects are tackled in this research. Firstly, the existing code construction technique is studied, and trying to find a more efficient method to construct the codes. Secondly, alternative detection techniques are investigated and compared to the existing ones. Thirdly, a software simulation of the SAC OCDMA system with the DW code family using the Virtual Photonics Instrument (VPI) Transmission Maker software version 7.1 is implemented.

A new code construction technique is proposed to overcome the drawbacks of the existing method, which is complicated and time consuming. Two equation-based code construction techniques are proposed. Both techniques provide a simplified and more efficient method of constructing codewords than the previous technique.

When the mapping technique is applied to increase the number of users for the DW code family, the SAC OCDMA detection (Complementary detection) cannot be used to retrieve desired signals due to unfixed cross-correlation between code sequences. A hybrid Wavelength Division Multiplexing/Spectral Amplitude Coding (WDM/SAC) system can be used to resolve this problem. A reduced set of Fiber Bragg Gratings (FBG) is proposed for the hybrid WDM/SAC to reduce cost and improve the performance. Theoretical calculations show an improvement for the proposed method over the hybrid WDM/SAC method.

Simulation results using VPI software show for the same transmission quality the proposed method can support longer transmission than the other methods.

TABLE OF CONTENT

| | |
|--|------|
| STATUS OF THESIS..... | i |
| APPROVAL PAGE | ii |
| TITLE PAGE | iii |
| DECLARATION | iv |
| ACKNOWLEDGEMENT | v |
| ABSTRACT | vi |
| TABLE OF CONTENT | viii |
| LIST OF TABLES | xii |
| LIST OF FIGURES | xiii |
| NOMENCULATURE..... | xv |
| CHAPTER ONE | 1 |
| 1. INTRODUCTION | 1 |
| 1.1 Background | 1 |
| 1.2 Telecommunication Networks | 1 |
| 1.3 Multiple Access Techniques | 2 |
| 1.4 Optical Code Division Multiple Access | 3 |
| 1.5 Problem statement..... | 5 |
| 1.6 Objectives | 6 |
| 1.7 Scope of study | 7 |
| 1.8 Methodology | 7 |
| 1.9 Thesis Overview | 8 |
| CHAPTER TWO | 9 |
| 2. OPTICAL CODE DIVISION MULTIPLE ACCESS SYSTEMS | 9 |
| 2.1 Introduction..... | 9 |
| 2.2 Coherent Optical CDMA Systems..... | 9 |
| 2.2.1 Pluse-Based Coherent DS-OCDMA..... | 9 |
| 2.2.2 Time Spread Optical CDMA (Weiner)..... | 11 |
| 2.2.3 Codes..... | 12 |

| | |
|--|----|
| 2.2.3.1 Walsh (Hadamard) Code..... | 12 |
| 2.2.3.2 Maximal-Length Code..... | 12 |
| 2.3 Incoherent Optical CDMA..... | 13 |
| 2.3.1 Incoherent Direct Spreading Optical CDMA | 13 |
| 2.3.1.1 Codes..... | 14 |
| 2.3.1.1.1 Optical Orthogonal Codes (OOC) | 14 |
| 2.3.1.1.2 Prime Code Family | 15 |
| 2.3.2 Wavelength Hopping/Time Spreading Optical CDMA Systems | 16 |
| 2.3.2.1 Codes..... | 16 |
| 2.3.2.1.1 Carrier Hopping Prime Code (CHPC)..... | 17 |
| 2.3.3 Spectral Amplitude Coding Optical CDMA Systems | 18 |
| 2.3.3.1 Codes..... | 19 |
| 2.3.3.1.1 Hadamard Code | 19 |
| 2.3.3.1.2 Modified Frequency Hopping Code | 20 |
| 2.3.3.1.3 The Double Weight Code Family | 22 |
| 2.4 Applications of Optical CDMA | 22 |
| 2.4.1 Optical CDMA in Metropolitan Area Networks | 22 |
| 2.5 Summary | 23 |
| CHAPTER THREE | 24 |
| 3. DOUBLE WEIGHT CODE FAMILY CONSTRUCTION | 24 |
| 3.1 Introduction..... | 24 |
| 3.2 Optical Codes Design | 24 |
| 3.3 The Double Weight (DW) Code..... | 25 |
| 3.4 The Modified Double Weight (MDW) Code..... | 26 |
| 3.4.1 Basic Matrix Construction Technique | 26 |
| 3.4.2 Mapping Technique | 29 |
| 3.5 Equation-Based Code Construction..... | 30 |
| 3.5.1 The First Equation..... | 30 |
| 3.5.1.1 Pattern Observation..... | 30 |
| 3.5.1.2 Construction of the General Equation..... | 31 |
| 3.5.2 The Second Equation | 33 |

| | |
|--|----|
| 3.5.2.1 Pattern Observation..... | 33 |
| 3.5.2.2 Construction of the General Equation..... | 34 |
| 3.6 Summary | 37 |
| CHAPTER FOUR..... | 38 |
| 4. PERFORMANCE ANALYSIS ON THE DETECTION SCHEME..... | 38 |
| 4.1 Introduction..... | 38 |
| 4.2 Multiple Access Interference (MAI)..... | 38 |
| 4.3 Noise Estimation..... | 39 |
| 4.3.1 Phase Induced Intensity Noise..... | 39 |
| 4.3.2 Shot Noise..... | 40 |
| 4.3.3 Thermal Noise..... | 40 |
| 4.4 Optical CDMA Systems | 41 |
| 4.5 Spectral Amplitude Coding Detection Schemes..... | 41 |
| 4.6 Double Weight Code Family Detection..... | 43 |
| 4.6.1 Complementary Detection Scheme..... | 43 |
| 4.6.1.1 Performance Analysis | 43 |
| 4.6.2 Hybrid Wavelength Division Multiplexing/Spectral Amplitude Coding | 49 |
| 4.6.2.1 Performance Analysis | 51 |
| 4.6.3 A Reduced Number of Fiber Bragg Gratings Approach | 53 |
| 4.6.3.1 Performance Analysis | 55 |
| 4.7 Simulation Setup..... | 56 |
| 4.8 Summary | 59 |
| CHAPTER FIVE | 61 |
| 5. RESULTS AND DISCUSSION..... | 61 |
| 5.1 Introduction..... | 61 |
| 5.2 Theoretical Results..... | 61 |
| 5.2.1 Comparison between the Complementary and the Hybrid WDM/SAC Methods..... | 61 |
| 5.2.2 Comparison between the Hybrid WDM/SAC and the Reduced FBGs Set Methods..... | 63 |
| 5.3 Simulation Results | 64 |

5.3.1 Eye Daigram 64

5.3.1 Distances Effect on Bit Error Rate68

5.4 Summary..... 69

6. CONCLUSION..... 70

6.1 Conclusion 70

6.2 Future Work..... 71

REFERENCES 72

PUBLICATIONS..... 77

APPENDIX A..... 78

APPENDIX B 81

LIST OF TABLES

| | |
|---|----|
| TABLE 1.1: COMPARISON BETWEEN TDMA, WDMA AND CDMA..... | 4 |
| TABLE 3.1: MDW OF WEIGHT FOUR ($W=4$) WITH MAPPING..... | 29 |
| TABLE 3.2: MDW OF WEIGHT SIX ($W=6$) WITH ONES PATTERN | 30 |
| TABLE 3.3: THE FABRICATED CODEWORD NUMBER 5 USING (3.16)..... | 33 |
| TABLE 3.4: MDW OF WEIGHT SIX ($W=6$) WITH BASIC BUILDING BLOCKS PATTERN..... | 33 |
| TABLE 3.5: MDW OF WEIGHT SIX ($W = 6$) WITH $[X1]$, $[X2]$ AND $[X3]$ | 34 |
| TABLE 3.6: THE FABRICATED CODEWORD NUMBER FIVE USING (3.27) WITH $[X1]$, $[X2]$ AND $[X3]$ | 36 |
| TABLE 3.7: THE FABRICATED CODEWORD NUMBER FIVE USING (3.27) WITH CHIPS REPRESENTATION | 37 |
| TABLE 4.1: MDW OF WEIGHT FOUR ($W=4$) WITH MAPPING..... | 49 |
| TABLE 4.2: CODE SEQUENCES FOR EACH USER IN THE SIMULATION..... | 56 |

LIST OF FIGURES

| | |
|--|----|
| Figure 1.1: TDMA, WDMA and CDMA. | 3 |
| Figure 1.2: General Scope of Study..... | 7 |
| Figure 2.1: Coherent DS-OCDMA System. | 10 |
| Figure 2.2: Coherent Time Spread–OCDMA Encoder..... | 11 |
| Figure 2.3: Incoherent DS-OCDMA Encoding/Decoding (a) Delay Lines (b) Programmable Ladders | 13 |
| Figure 2.4: Incoherent Frequency Hopping/Time spreading OCDMA System | 17 |
| Figure 2.5: Incoherent Spectral Amplitude Coding OCDMA System | 18 |
| Figure 3.1: General Form for MDW basic matrix construction | 27 |
| Figure 4.1: Complementary Detection Scheme | 42 |
| Figure 4.2: SAC System for Non-Complementary Codes..... | 42 |
| Figure 4.3: Complementary SAC decoder using FBGs..... | 43 |
| Figure 4.4: PSD of the Received Signal $r(v)$ | 46 |
| Figure 4.5: Structure of (a) Encoder and (b) Decoder for user number 1 using MDW with mapping using FBGs..... | 50 |
| Figure 4.6: Structure of proposed reduced set of FBGs decoder for user number 1 using MDW ($w=4$) with mapping..... | 53 |
| Figure 4.7: Transmitter Design for MDW code ($w=4$) system..... | 57 |
| Figure 4.8: Receiver Design for Complementary SAC system | 57 |
| Figure 4.9: Receiver Design for Hybrid WDM/SAC system using FBGs | 58 |
| Figure 4.10: Receiver Design for Reduced set of FBGs for Hybrid WDM/SAC system | 58 |
| Figure 4.11: Network Setup for four users | 59 |
| Figure 5.1: SNR versus the number of active users for Complementary and hybrid WDM/SAC. | 62 |
| Figure 5.2: BER versus the number of active users for Complementary and hybrid WDM/SAC | 62 |
| Figure 5.3: BER versus the number of active users for hybrid WDM/SAC and reduced set of FBGs | 63 |
| Figure 5.4: Eye Diagram for MDW Code with Complementary SAC at 2.5 Gbps | 64 |

| | |
|---|----|
| Figure 5.5: Eye Diagram for MDW Code with Hybrid WDM/SAC at 2.5 Gbps..... | 65 |
| Figure 5.6: Eye Diagram for MDW Code with Reduced set of FBGs for Hybrid WDM/SAC at 2.5 Gbps | 65 |
| Figure 5.7: Eye Diagram for MDW Code with Complementary SAC at 10 Gbps | 66 |
| Figure 5.8: Eye Diagram for MDW Code with Hybrid WDM/SAC at 10 Gbps..... | 67 |
| Figure 5.9: Eye Diagram for MDW Code with Reduced set of FBGs for Hybrid WDM/SAC at 10 Gbps | 67 |
| Figure 5.10: BER versus Distance for MDW Code with Hybrid WDM/SAC and reduced set of FBGs at 10 Gbps | 68 |

NOMENCULATURE

| | |
|----------|---|
| B | Noise Equivalent Electrical Bandwidth |
| e | Electrons Charge |
| $G(\nu)$ | Single Sideband Power Spectral Density |
| h | Planck's constant |
| K_b | Boltzmann's Constant |
| P_{sr} | Effective Power of a Broadband Source |
| R_L | Receiver Load Resistance |
| T | Absolute Temperature |
| T_n | Absolute Receiver Noise Temperature |
| $u(\nu)$ | Unit Step Function |
| ν_c | Central Frequency of the Original Broadband Optical Pulse |
| ν_0 | Central Optical Frequency |

GREEK SYMPOLS

| | |
|-------------|------------------------------|
| $\Delta\nu$ | Optical Source Bandwidth |
| τ_c | Coherence Time of the Source |
| η | Quantum Efficiency |

\mathfrak{R} Responsivity of the Photodetectors

λ_a Auto Correlation

λ_c Cross Correlation

CHAPTER ONE

INTRODUCTION

1.1 Background

As the demand of Telecommunication systems and Networks to provide multimedia and other broadband integrated services is growing [1-6], development in the corresponding electronics and transmission media is crucial. The development of fiber optics communication in the last few years has made the optical fiber a strong contender for the modern telecommunication systems [1-6].

Optical fiber provides extremely high bandwidth (in Tbps) if compared to the traditional transmission media [6]. The other traditional media struggle to reach the Giga mark. The attenuation factor is much less in optical fiber [1-6], which enables use for longer distance transmission without the need for amplification or regeneration. Due to the usage of light as a carrier, many different wavelengths can be multiplexed on the same fiber in order to increase the overall bandwidth. As a result, it will reduce cost and also enable multiple user access.

1.2 Telecommunication Networks

Telecommunication networks can be divided into two major categories:

1. Long-haul networks:

Long-haul networks, Backbone networks or Wide Area networks are networks which cover broad geographic areas (Thousands of kilometers). WANs are usually setup by services providers or telephone companies, expensive equipment is required to optimize transmission.

2. Short-haul Networks:

Short-haul networks are divided into two categories:

- I. Local Area Networks: these networks have a limited coverage that does not extend beyond a few hundred meters, usually used in buildings and college campuses.
- II. Metropolitan Area Networks: these cover distances of a few kilometers. These networks are used to connect different parts of a city together. Multiple routers, switches and hubs are used in MANs.

1.3 Multiple Access Techniques

Multi access is a scheme to share a common communication resource among a number of users. The main challenge in modern telecommunication systems is to efficiently divide the available transmission bandwidth among different users and obtain maximum utilization.

Optical fibers provide a very high transmission bandwidth, which allows multi users to simultaneously access the shared medium. A multiple access technique is required for combining and separating traffic on a shared physical medium.

There are three multi access techniques; Time Division Multiple Access (TDMA), Wavelength Division Multiple Access and Code Division Multiple Access. TDMA and WDMA are traditionally used in fiber optics communication systems to allocate the available bandwidth among the different users. TDMA operates by allocating each user with a specific timeslot, and each user transmits and receives its data within this timeslot. WDMA systems allocate different users with different wavelengths around a center wavelength. TDMA and WDMA systems allocate a permanent timeslot or wavelength channels to different users respectively. However, this can lead to bandwidth wastage if not all the users are using the network. A more efficient multi access for bursty traffic is CDMA, where each user is given a unique codeword to differentiate him from other users. Figure 1.1 shows the three multi access schemes.

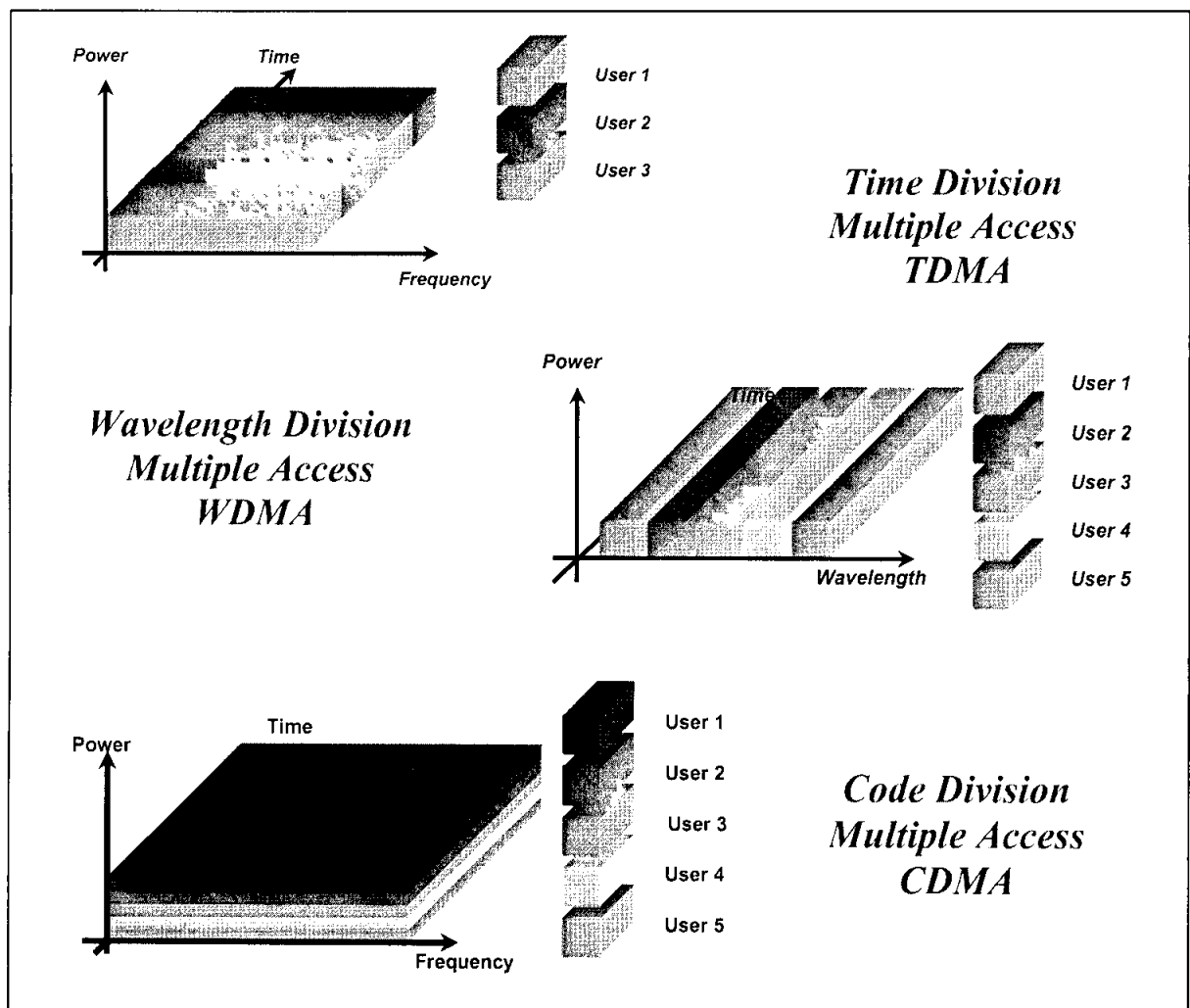


Figure 1.1: TDMA, WDMA and CDMA

1.4 Optical Code Division Multiple Access

Optical CDMA or OCDMA is an interesting development in short-haul optical networking because it can support both wide and narrow bandwidth applications on the same network. In addition, it connects large number of asynchronous users with low latency and jitter and therefore permitting quality of service guarantees to be managed at the physical layer. Moreover, it also offers robust signal security and has simplified network topologies. However, for improperly designed codes, the maximum number of simultaneous users and the performance of the system can be seriously limited by the multiple access interference (MAI) or crosstalk from other users. The optical signal

carrying the data exhibits a set of signal processing operations. Hence this modifies its time and/or frequency appearance, in a way recognizable only by the intended receiver. Otherwise, only noise-like bursts are observed. A comparison between the three different multi access techniques is given in TABLE 1.1.

TABLE 1.1:
COMPARISON BETWEEN TDMA, WDMA AND CDMA.

| MULTIPLE ACCESS SCHEMES | ADVANTAGES | DISADVANTAGES |
|-------------------------|--|--|
| 1. TDMA | 1. Dedicated timeslots provided 2. High throughput 3. Deterministic access | 1. Accurate synchronization needed 2. Not efficient in bursty traffic 3. Bandwidth wasted 4. Performance degrades with the number of simultaneous users |
| 2. WDMA | 1. Dedicated channels provided | 1. Channel crosstalk 2. Bandwidth wasted 3. Low bandwidth efficiency 4. Non-linear effects |
| 3. CDMA | 1. Simultaneous users allowed 2. Asynchronous access 3. No delay or scheduling 4. High bandwidth efficiency 5. Efficient for bursty traffic. 6. Dedicated channels provided | a. Multiple Access Interference (MAI) |

1.5 Problem Statement

Due to the success of CDMA in wireless communication, researchers are adapting this technique to the optical world under the motivation of accommodating a larger number of clients to communicate simultaneously through a common optical fiber.

Optical CDMA started around two decades ago [7]. In the beginning researchers tried to apply the same CDMA techniques already established in wireless communication. The results that they obtained were far from comparable to the success of that in the wireless [8-9]. This is mainly due to the fundamental difference between the radio frequency and optical fiber communication environments. For instance, the output characteristics of an optical source, such as phase and polarization, are not controllable as of a microwave source. The optical fiber exhibits phenomena that are either not present or insignificant in, the RF channel. Also, the photodetector detects incident power only, while the phase and polarization cannot be easily sensed. A complex architecture is required in order to control and detect such parameters and it is inappropriate for an access communication system. To overcome these difficulties researchers have been trying to establish newer encoding and decoding techniques [10-30]. Many different techniques have been proposed and these techniques will be studied in chapter two. Another limitation is optics to electronics and electronics to optics conversion, which limits the transmission speed. A modern approach is to use an all optics processing scheme (optical signal processing) [10-11].

Due to the numerous drawbacks of TDMA and WDMA, Optical CDMA appears to be the best alternative technique to support short-haul transmission, where the number of simultaneous users is high, and there is asynchronous access and bursty traffic.

The two major factors that affect the performance of the OCDMA system are code design and receiver design or the detection technique used []. Many codes have been proposed for different OCDMA systems. For conventional time spreading OCDMA systems [12-13], Optical Orthogonal Codes (OOC) [12-13] and Prime Codes [14] have been proposed. For the wavelength-hopping time-spreading OCDMA system, Carrier hopping

[14], and Extended Carrier Hopping Prime codes [15] have been proposed. For the Spectral Amplitude Coding (SAC) OCDMA system [16], m -sequences [17], Hadamard [18], Balanced Incomplete Block Design (BIBD) code, Modified Quadratic Congruence (MQC) code, Modified Frequency Hopping (MFH) code [19], and most recently the Double Weight (DW) code family have been proposed [20].

In this thesis, the most recently developed code in SAC systems, the Double Weight (DW) code family is studied. A new equation based code construction technique is proposed. The effect of incrementing the number of users using the mapping technique on the detection scheme is also analyzed and simulated.

1.6 Objectives

The main goal of this research is to enhance the performance of the DW code family to give better results. The objectives of this research include:

1. To find a new equation-based construction technique for the DW code family.
2. To derive equations for the codeword construction and code length.
3. To find an alternative detection technique to support user increment using the mapping technique.
4. To enhance the alternative detection scheme by reducing cost and improving performance.

1.7 Scope of Study

In this research, multiple access and multiplexing issues are focused on through studies performed at the physical layer. Optical CDMA is a new multi access technique, which promises better performance for short-haul optical fiber networks. This research concentrates on the DW code family as the most recently developed code for SAC OCDMA systems. Figure 1.2 shows the study structure of this research. Three main subjects will be considered, code construction, detection techniques and software simulation.

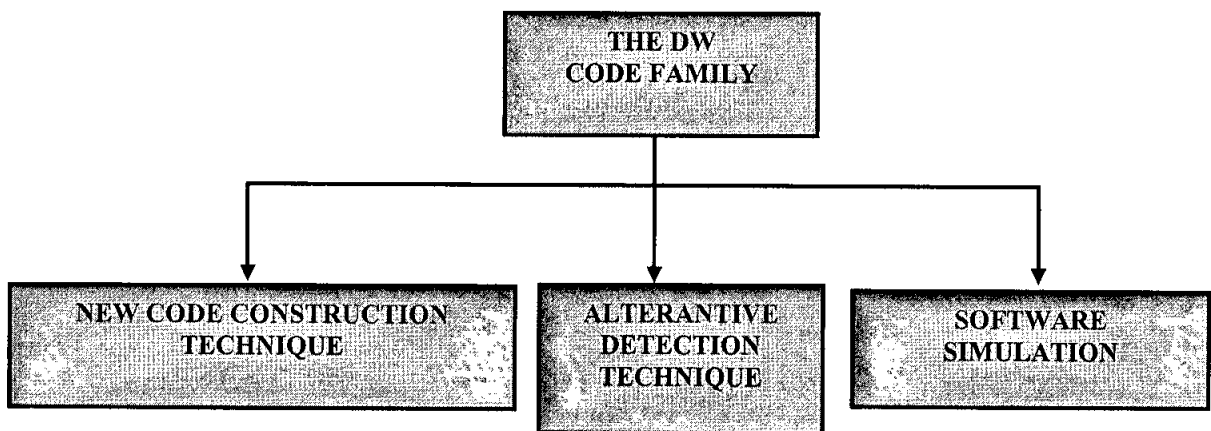


Figure 1.2: General Scope of Study

1.8 Methodology

The motivation of this research is to enhance the DW code family to give a better overall performance. Three aspects are covered in this research. Firstly, the study of the existing code construction technique, the Matrix construction and the Mapping technique, and try to find a more efficient method of constructing the codes. Secondly, alternative detection techniques are investigated and compared to the existing ones. Thirdly, a software simulation of a SAC Optical CDMA system with the DW code family using the Virtual Photonics Instrument (VPI) transmission maker software version 7.1 is implemented.

A software implementation of the whole system is built and used to study the performance of the code. A software simulation is important since it normally considers all practical factors which may be too extensive to be considered in the theoretical development. For example, the effects of material dispersion, fiber nonlinearities and insertion loss are not considered in the theoretical development.

1.9 Thesis Overview

Chapter One gives a general view of the fiber optic communication and optical CDMA systems. Problem statements, objectives and scope of study are also outlined.

Chapter Two concentrates on the different Optical CDMA systems. Examples of the different systems and the codes used for each system are given.

Chapter Three covers the construction of the DW code family. The existing technique is studied and a new construction technique is proposed.

Chapter Four focuses on the detection scheme for the DW code family and the effects of increasing the number of users on the correlation properties and on the performance.

Chapter Five shows the results obtained through theoretical calculations and software implementation.

Chapter Six gives concluding remarks and future work.

CHAPTER TWO

OPTICAL CODE DIVISION MULTIPLE ACCESS SYSTEMS

2.1 Introduction

In this chapter, different Optical CDMA systems are discussed. Optical CDMA can be divided into two major categories which are coherent systems and incoherent systems. Coherent systems are more complex and need more sophisticated and expensive equipment than incoherent systems.

2.2 Coherent Optical CDMA systems

In coherent systems, the complex nature of the optical field is taken into account in the encoding process including amplitude and phase. Phase plays an important role in code design. Manipulation in the optical field phase and amplitude allows the sum of the cross-correlation property to be zero.

There are many coherent optical CDMA systems, two examples of which are pulse-based coherent direct spread CDMA and time spread optical CDMA.

2.2.1 Pulse-Based Coherent DS-OCDMA

The development of femtosecond Mode Locked Lasers (MLL) delivering a train of ultra-short pulses with high coherence purity has motivated the emergence of new all-optical CDMA techniques. Each pulse is modulated by the value of the OOK data, and then split into identical sub-pulses along different optical paths. A combiner gathers all the sub-pulses into the same fiber. The lengths of the optical paths are dimensioned so that the sub-pulses will be placed corresponding to a pre-determined pattern or code. The splitters are separated by a distance fixing the time spacing between the chip pulses. The phase of

each tapped pulse is changed by an optical phase shifter consisting of an optical waveguide and a heater. The phase shifters adjust the tapped pulses as prescribed by the bipolar code. Tapped pulses are given a corresponding phase shift [21].

At the receiver, a similar setting is configured in order to match the desired user's encoded signal. The correlation between the receiver code and the desired user code leads to an auto-correlation peak. The interference signals, however, contribute by low-level peaks. Once decoded, the receiver may require some important and complex processing operations. This complexity is mainly due to the incapacity of electronics to make the very high speed processing required to finalize the reception operation. The decoded signal should be compared to a threshold level in order to decide about the data bit value. The threshold value can be estimated using the statistics of the family of codes, and the number of active users. Furthermore, the desired part of the signal exists in a chip duration, over which integration should be performed. Since the original optical pulses are of sub-picosecond duration, it is not realistic to perform such operations in the electric domain. Figure 2.1 shows the encoder/decoder of Pulse-Based Coherent DS-OCDMA system.

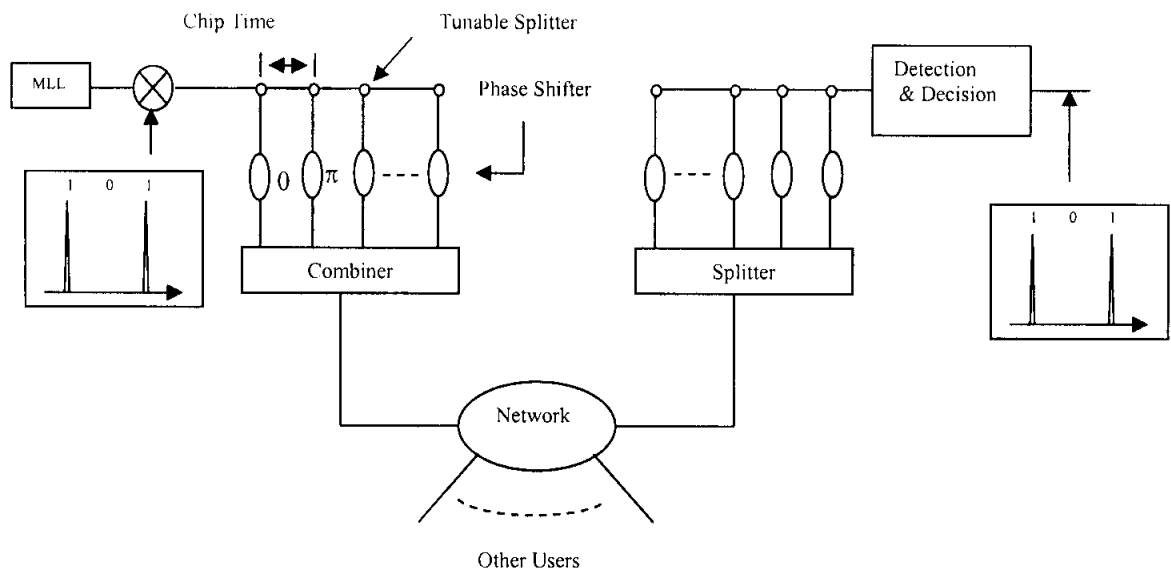


Figure 2.1: Coherent DS-OCDMA System

2.2.2 Time Spread Optical CDMA (Weiner)

Time spread-CDMA, developed by Weiner [10,22-27] in the early 90s, is considered among the most attractive alternatives (see Figure 2.2). This was the first time that the frequency axis itself was used as an encoding resource. This required an ultra-short pulse mode locked laser providing a coherent broad bandwidth. The MLL output is modulated by the binary data in OOK format. The signal is then focused on a diffraction grating, which spatially deploys the frequency components of the pulse. A programmable Liquid Crystal Modulator (LCM) phase mask introduces a phase-shift of 0 or π at each spectral component according to a given bipolar frequency code. Following the mask, the frequencies are gathered using a second diffraction grating and injected into the fiber. The setting, including a phase mask, two lenses, and gratings, is usually referred to as a $4F$ -diagram [22-27].

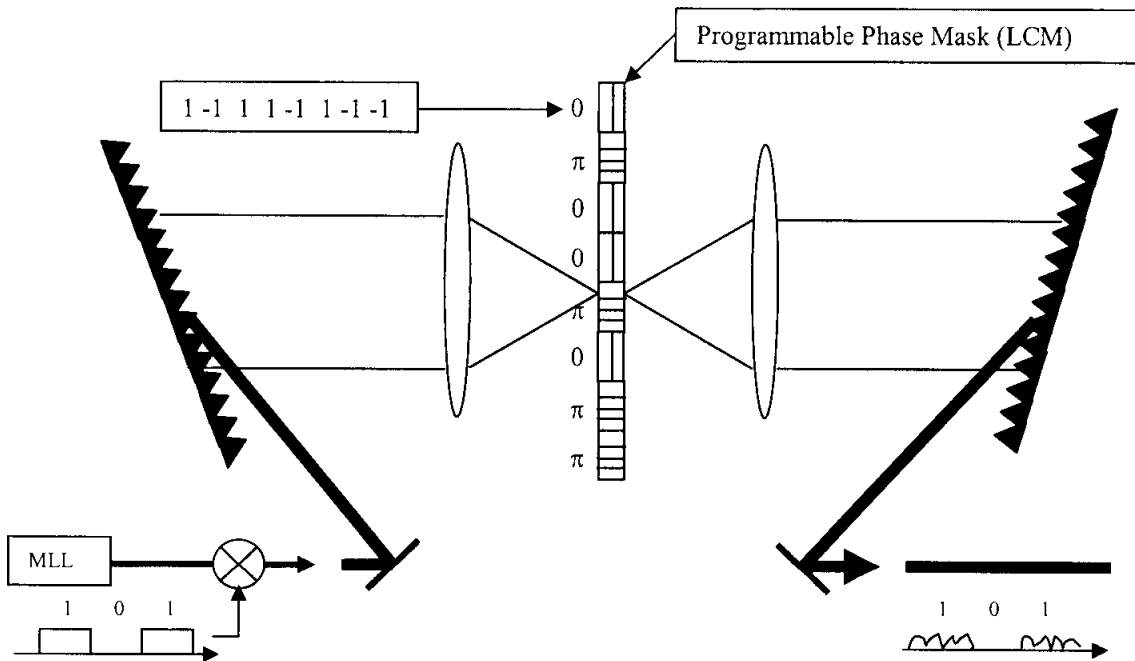


Figure 2.2: Coherent Time Spread-OCDMA Encoder

2.2.3 Codes

The same bipolar codes used in wireless communication are used here [28-29]. The bipolar codes used in wireless CDMA are designed to have close-to-zero cross-correlation function to minimize MAI. The most popular codes are the Walsh (Hadamard) code and pseudorandom sequences as maximal length sequences.

2.2.3.1 Walsh (Hadamard) code

Walsh (Hadamard) codes are employed to improve the bandwidth efficiency of wireless CDMA since they have zero cross-correlation function when they are all synchronized in time [28]. Hadamard codes have length of $N = 2^n$, denoted by H_N^j , where n is a positive integer, $j \in [0, N-1]$ is the j th row extracted bipolar sequence of H_N .

$$H_1 = [1], H_2 = \begin{bmatrix} 1 & 1 \\ 1 & -1 \end{bmatrix}, H_3 = \begin{bmatrix} H_2 & \overline{H_2} \\ H_2 & \overline{H_2} \end{bmatrix} = \begin{bmatrix} 1 & 1 & 1 & 1 \\ 1 & -1 & 1 & -1 \\ 1 & 1 & -1 & -1 \\ 1 & -1 & -1 & 1 \end{bmatrix} \quad (2.1)$$

$$H_{2^{n+1}} = \begin{bmatrix} H_{2^n} & \overline{H_{2^n}} \\ H_{2^n} & \overline{H_{2^n}} \end{bmatrix} \quad (2.2)$$

where $\overline{H_{2^n}}$ represents the complement of H_{2^n} . The cross-correlation of any two code sequences is zero ($H_N^{(j)}(H_N^{(k)})^T = 0$) and the auto-correlation for the same code sequence is N ($H_N^{(k)}(H_N^{(k)})^T = N$).

2.2.3.2 Maximal-Length Sequences

The maximal-length sequences can be expressed as $S_m = [c \ c^{(-1)} \ c^{(-2)} \ \dots \ c^{(-i)} \ \dots \ c^{(-2^m+2)}]^T$ for a length $2m-1$, where $c^{(-i)}$ represents the i th cyclic left-shift of c , and T the vector transpose. For a code sequence $c = [+1 \ +1 \ -1 \ +1 \ -1 \ -1 \ -1]$, $c^{(-1)} = [+1 \ -1 \ +1 \ -1 \ -1 \ -1 \ +1]$...etc [28-29].

2.3 Incoherent Optical CDMA

Incoherent systems do not exploit the complex optical field. This type of system mainly depends on the amplitude in code design. Incoherent systems have attracted a significant body of research over the last two decades. There are three main systems that have been proposed; Direct Spreading Optical CDMA, Spectral Amplitude Coding systems and Frequency Hopping systems.

2.3.1 Incoherent Direct Spreading Optical CDMA

This system depends on direct spreading with unipolar codes [12-13,30-39]. Figure 2.3 shows an incoherent DS-OCDMA system. Earlier systems used tap delay lines for the encoder and decoder design. However, programmable ladder networks are more attractive nowadays.

The receiver decoder is identical to the encoder except that it performs the inverse function. Chip-pulses arriving in advance are delayed so that all the chip-components of the signal travel an equivalent path. The pulses coming from the desired transmitter will superpose in the same chip duration, thus requiring a fast time-gate.

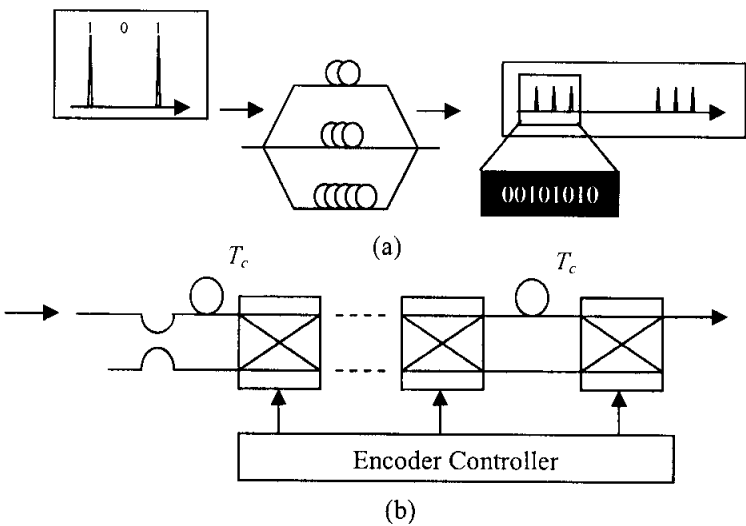


Figure 2.3: Incoherent DS-OCDMA Encoding/Decoding (a) Delay Lines (b) programmable ladders

2.3.1.1 Codes

There have been many codes invented for Direct Spread OCDMA systems, the most popular of which are the Optical Orthogonal Codes [12-13,30-35] and the Prime Codes Family [36-39].

2.3.1.1.1 Optical Orthogonal Codes (OOC)

The Optical Orthogonal Codes (OOC) were first invented by Salehi and Brackett [12-13], and they are the most efficient codes in DS-OCDMA. The OOCs are a sequence of (0,1) and have a general code construction of $(L, w, \lambda_a, \lambda_c)$, where L is code length, w is the code weight, λ_a is the auto-correlation property and λ_c is the cross-correlation property.

OOCs are designed to have the following correlation properties:

- I. Autocorrelation property: for any $X \in C$ and any integer τ , $0 \leq \tau \leq L$

$$\sum_{i=0}^{L-1} X_i X_{i \otimes \tau} \leq \lambda_a \quad (2.3)$$

- II. Cross correlation property for any $X \neq Y \in C$ and any integer τ

$$\sum_{i=0}^{L-1} X_i Y_{i \otimes \tau} \leq \lambda_c \quad (2.4)$$

where \otimes denotes modulo L

The OOCs have correlation values of $\lambda_a = \lambda_c \leq 1$. Through these correlation properties it can be seen that it is easy to distinguish a code sequence in the presence of other code sequences and shifted versions of the same code sequence.

The relation between the number of users K , the weight w and the code length L is:

$$K = \frac{L - 1}{w(w - 1)} \quad (2.5)$$

There are three methods used to construct OOCs :

1. The Interactive Construction Technique.
2. The Greedy Algorithms Technique
3. The Projective Geometry Technique.

The projective geometry technique is the most popular construction method. There are several mathematical approaches using the projective geometry technique to design the OOCs [32]. An example of the OOC(341, 5, 1) is given in the Appendix A.

The disadvantages of the OOCs are that they have very large code sequences to support even a moderate number of clients. Also, all three techniques used in the code construction are complex and require extra system memory to store constructed codes beforehand.

2.3.1.1.2 Prime Code Family

The prime code was the first code implemented in optical CDMA [14,36-38]. The number of code sequences in the prime code over Galois field $GF(p)$ of a prime number p is p . the code length is p^2 .

With $GF(p) = \{0, 1, 2, \dots, p-1\}$, a Prime sequence $S_i = (s_{i,0}, s_{i,1}, \dots, s_{i,(p-1)})$ is constructed by multiplying every element j of $GF(p)$ by an element i of $GF(p)$ modulo p ,

Therefore,

$$s_{i,j} = (i \cdot j) \otimes p \quad \text{for } i, j = \{0, 1, 2, \dots, p-1\} \quad (2.6)$$

p distinct prime sequences can be obtained.

The prime sequences can be mapped into a binary code sequence using $C_i = (c_{i,0}, c_{i,1}, \dots, c_{i,k}, \dots, c_{i,p^2-1})$ by assigning ones in positions $i = s_{i,j} + jp$ and zeros in all other positions.

Therefore,

$$c_{i,k} = \begin{cases} 1 & \text{for } k = s_{i,j} + jp, \quad j = 0, 1, \dots, p-1 \\ 0 & \text{Otherwise} \end{cases} \quad (2.7)$$

For $i = 0, 1, \dots, p-1$.

The prime code has a high auto-correlation equal to the prime number and a cross-correlation less than two. The main disadvantages of the prime code are that weight is always equal to a prime number and it has high auto-correlation sidelobes, which makes it difficult to distinguish the code sequence from shifted versions of itself.

To solve these problems, new codes from the prime code family have been invented such as the Extended prime code, the Generalized prime code, the $2n$ prime code ...etc [14]. An example of the prime code for $GF(5)$ is given in Appendix A.

2.3.2 Wavelength Hopping/Time Spreading Optical CDMA Systems

To support large number of users in DS-OCDMA systems, codes with very long code length are needed to give good correlation properties. In other words, a very large bandwidth is required, creating a stringent requirement for encoding and decoding hardware speed.

Tancevski and Andonovic [39-40] proposed to imbed multiple wavelengths inside the optical code, making a second degree of coding dimension [41]. This approach can be viewed as a frequency or wavelength hop that takes place at each pulse of the code sequence, assuming that the number of wavelength available is equal or higher than the code weight. Figure 2.5 shows the frequency hopping/time spreading OCDMA system.

2.3.2.1 Codes

Two dimension codes have been invented for frequency hopping systems. The most popular codes are the Carrier Hopping Prime Code, the Multilength Carrier Hopping Code [14] and the Extended Carrier Hopping Prime Code [15].

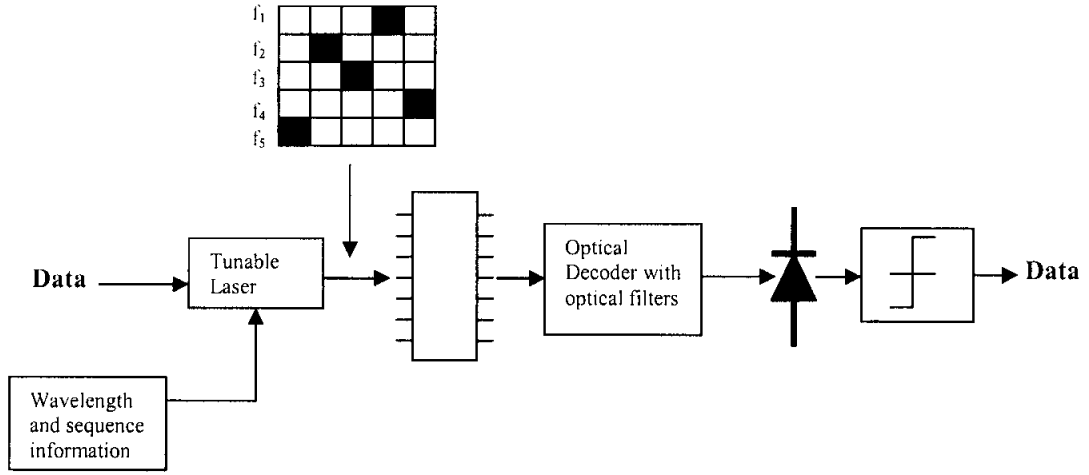


Figure 2.5: Incoherent Frequency Hopping/Time spreading OCDMA System

2.3.2.1.1 Carrier Hopping Prime Code (CHPC)

The carrier hopping prime code (CHPC) uses a two-dimensional approach. In which the code sequences are represented both in time and wavelength. The CHPC has general representation of $w \times p_1 p_2 \dots p_k$ binary matrices of length $p_1 p_2 \dots p_k$, weight w , and a cardinality of $p_1 p_2 \dots p_k$, where $p_k \geq p_{k-1} \geq \dots \geq p_2 \geq p_1 \geq w$. The weight w is the number of rows, and it is related to the number of available carriers. $p_1 p_2 \dots p_k$ is the number of columns, and its related to the length of the carrier hopping matrices. Because each matrix has a single pulse '1' per row and each pulse is assigned to a different carrier, the CHPC has auto-correlation sidelobes of zero and a maximum cross-correlation of one.

The general construction of the CHPC is:

$$\left\{ \left[\begin{aligned} &(0,0), (1, i_1 + i_2 p_1 + \dots + i_k p_1 p_2 \dots p_k), \\ &\left(2, 2 \otimes_{p_1} i_1 + \left(2 \otimes_{p_2} i_2 \right) p_1 + \dots + \left(2 \otimes_{p_k} i_k \right) p_1 p_2 \dots p_{k-1} \right) \dots \\ &\left(w-1, (w-1) \otimes_{p_1} i_1 + \left((w-1) \otimes_{p_2} i_2 \right) p_1 + \dots + \left((w-1) \otimes_{p_k} i_k \right) p_1 p_2 \dots p_{k-1} \right) \end{aligned} \right] : \right. \quad (2.8) \\ \left. i_1 = \{0, 1, \dots, p_1 - 1\}, i_2 = \{0, 1, \dots, p_2 - 1\}, \dots, i_k = \{0, 1, \dots, p_k - 1\} \right\}$$

The multilength carrier hopping prime code supports a large variety of services (data, voice, image and video) for users with different signaling and quality of services [14].

The extended carrier hopping prime code was invented to achieve higher cardinality than the original CHPC [15,42]. An example of the CHPC for $(8 \times 41, 8, 0, 1)$ for users 4, 9, 11 and 22 is given in the Appendix A.

2.3.3 Spectral Amplitude Coding Optical CDMA Systems

This approach was first introduced by Zaccarin and Kavehrad [16-17,43-44]. Spectral Amplitude Coding SAC OCDMA systems have been introduced to minimize the multi access interference present in the incoherent DS-OCDMA system. This approach is similar to the coherent phase encoded system in the sense that the frequency components from a broadband optical source are resolved first. Each code channel then uses a spectral amplitude encoder to selectively block or transmit certain frequency components as in Figure 2.4.

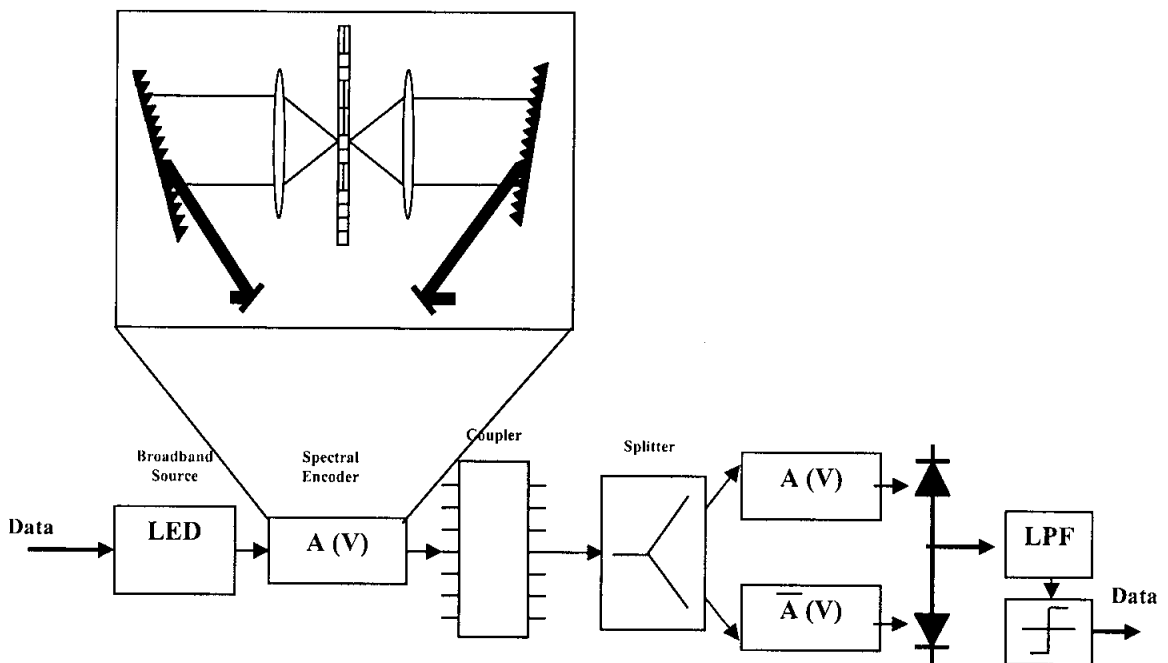


Figure 2.4: Incoherent Spectral Amplitude Coding OCDMA System

A balanced receiver with two photodetectors is used as part of the receiver. The receiver filters the incoming signal with the same spectral amplitude filter also called the direct filter used at the transmitter as well as its complementary filter. The outputs from the complementary filters are detected by the two photodetectors connected in a balanced

fashion. For an unmatched transmitter, half of the transmitted spectral components will match the direct filter and the other half will match the complementary filter. Since the output of the balanced receiver represents the difference between the two photodetector outputs, unmatched channels will be cancelled, while the matched channel is demodulated.

Since there is a subtraction between two photodetectors, it is possible to design codes so that full orthogonality can be achieved with the incoherent spectral intensity encoding approach. In principle, orthogonality eliminates the crosstalk or multiple access interference from other users. Bipolar signaling can also be obtained by sending complementary spectrally encoded signals [18].

Besides using Diffraction Gratings, Fiber Bragg Gratings (FBG) and Array Waveguide Gratings (AWG) can be used in the encoder and decoder design for unipolar codes systems.

2.3.3.1 Codes

There have been many codes proposed for SAC OCDMA systems. The codes proposed for SAC OCDMA have a fixed in-phase cross-correlation, such as the unipolar versions of the Maximal-Length code [17] and the Hadamard code [18]. Recently, codes that have ideal in-phase cross correlation ($\lambda_c = 1$) have been proposed. These codes are the Balanced Incomplete Block Design (BIBD) code [45], the Modified Quadratic Congruence (MQC) code [46], the Modified Frequency Hopping (MFH) code [47] and, most recently the Double Weight (DW) code family [20,48].

2.3.3.1.1 Hadamard Code

The Hadamard code and Maximal-Length code used in incoherent SAC OCDMA systems are driven from coherent counterparts by substituting ‘-1’ by ‘0’ in the code sequences. These codes are called complementary codes because the code sequence is sent to represent binary data ‘1’ (mark) and the complementary of the code sequence is sent to represent binary data ‘0’ (space).

The Hadamard code is represent by:

$$H_1 = [1], H_2 = \begin{bmatrix} 1 & 1 \\ 1 & 0 \end{bmatrix}, H_3 = \begin{bmatrix} H_2 & \overline{H_2} \\ H_2 & \overline{H_2} \end{bmatrix} = \begin{bmatrix} 1 & 1 & 1 & 1 \\ 1 & 0 & 1 & 0 \\ 1 & 1 & 0 & 0 \\ 1 & 0 & 0 & 1 \end{bmatrix} \quad (2.9)$$

The Hadamard code will support $2^n - 1$ subscriber because the first code sequence is all ones, it's not taken into account. The main disadvantage of the Hadamard code is that is there a wastage of code sequences because the code sequences are always $2^n - 1$. Also, the cross-correlation is high ($N/2$), which causes the presence of a dominant source of noise in SAC OCDMA systems known as the Phase Induced Intensity Noise (PIIN).

2.3.3.1.2 Modified Frequency Hopping Code

The BIBD code, MQC code, MFH code and the DW code family are non-complementary codes because nothing is sent to represent a space or binary data '0'. The construction of the MFH code is given below [47]:

a. Step 1:

Let $GF(q)$ denote a finite field of elements and β is a primitive element of $GF(q)$. A number sequence $y_{a,b}(k)$ can constructed with elements of $GF(q)$ using the following expression:

$$y_{a,b}(k) = \begin{cases} \beta^{(\alpha+k)} + b, & k = 0, 1, 2, \dots, q-2 \\ b, & k = q-1 \\ \alpha, & k = q \end{cases} \quad (2.10)$$

Where α and b are elements of $GF(q)$ expressed by $\alpha \in \{0, 1, 2, \dots, q-2\}$ and $b \in \{0, 1, 2, \dots, q-1\}$. The parameters α and b are fixed for each specified number sequence and their changes result in different sequences. It should be noted that the operations in (2.10) are determined by $GF(q)$.

Because the values of β^k are not equal to zero no matter what the value of k is, the first elements of each sequence are all different and they can exactly constitute a whole set of $GF(q)$. Another sequence can be added into the new code family without affecting the ideal in-phase cross correlation of the final binary code.

These number sequences are constructed using the following expression:

$$y'(k) = \begin{cases} b, & k = 0, 1, 2, \dots, q-1 \\ q-1, & k = q. \end{cases} \quad (2.11)$$

Therefore, a full set of q^2 number sequences is obtained which is denoted by $y(k)$ in the rest of this section.

b. Step 2:

Based on each generated number sequence $y(k)$, construct a sequence of binary numbers $s(i)$ by using the mapping method as in (2.14)

$$s(i) = \begin{cases} 1, & \text{if } i = kp + y(k) \\ 0, & \text{else} \end{cases} \quad (2.12)$$

Where $i = 0, 1, 2, \dots, q^2 + q - 1$ and $k = \lfloor i / q \rfloor$.

MFH code possesses the following properties.

- a. Each code sequence $q^2 + q$ has elements that can be divided into $(q+1)$ groups, and each group contains one “1” and $(q-1)$ “0”s.
- b. In-phase cross correlation between any two sequences is always equal to 1.

In the Appendix, some code examples for different values of parameters α and b are listed when q is equal to 2^2 (i.e. $q = 4$). Here the selected primitive irreducible polynomial is written as $x^2 + x + 1$ and the primitive element β is (10) in binary form, which can be represented as ‘2’ in the decimal system [47].

2.3.3.1.3 The Double Weight Code family

The DW code family is the most recent code family developed for SAC OCDMA systems [20,48]. The DW code family will be studied in detail in the next chapter.

2.4 Applications of Optical CDMA

As the desire to make more use of the optical fiber bandwidth is increasing, Code Division Multiple Access (CDMA) emerges as a promising multi access technique [7]. From its name, CDMA is a multiplexing scheme based on the principle of message encoding and decoding by authorized receivers only and in the presence of interfering signals from network other users. Due to its support for asynchronous access and coding capabilities, CDMA is gaining more and more attention in the optical communication world compared to its more established counterparts. Moreover, there is the prospect of performing an all optical encoding/decoding process (optical signal processing), and therefore achieving real transparent networks, which could potentially lead to network throughput of the rate of Tbps [50]. A major field of application for Optical CDMA is short-haul area networks and more precisely Metropolitan area networks.

2.4.1 Optical CDMA in Metropolitan Area Networks

A Metropolitan Area Network (MAN) is a network that covers an area of 10 – 100 km in diameter. A MAN can range from a group of buildings to a group of cities. The MAN can function as an intermediate bridge between Local Area Networks (LANs) and Wide Area Networks (WANs). One end is called the central office (CO) of a MAN which is connected to a WAN or long-haul infrastructure and the other ends are called nodes which are connected to LANs and the end users.

Recently, as the number of users accessing MANs is increasing and the demand for high capacity in optical networks to support new generation information services such as Internet, multimedia, and video conferencing is getting higher, researchers are adopting Optical CDMA to be used in MANs, as Optical CDMA can support large numbers of

asynchronous users compared to other multi access techniques. Also the bursty traffic nature of MANs is suited to Optical CDMA.

2.5 Summary

In this chapter, different Optical CDMA systems were covered. Examples of Coherent systems such as Pulse-Based Coherent DS-CDMA and Time Spread Optical CDMA were discussed. Examples of Incoherent systems were given such as Direct Spreading Optical CDMA, Wavelength Hopping/Time Spreading Optical CDMA and Spectral Amplitude Coding Optical CDMA. Also examples of the frequently used codes for each system were discussed. This chapter also covered some of the optical CDMA applications on MANs.

CHAPTER THREE

DOUBLE WEIGHT CODE FAMILY CONSTRUCTION

3.1 Introduction

In this chapter, the Double Weight (DW) code family is studied in detail. This chapter starts with a general overview of codes. Then the DW code family code construction is focused on. The existing technique, the matrix construction and mapping technique for DW family code construction are analyzed. A new equation based code construction technique is proposed for the DW code family to overcome the drawbacks of the existing technique. Two equations are proposed; the first is based on the distribution of ones '1' in each codeword and the second is based on the basic building blocks of the basic matrix. The proposed new technique is accurate, fast and precise in constructing codewords for each client.

3.2 Optical codes Design

Any OCDMA code can be represented in a general form of (L, w, λ_c) [12-13], where L is the code length, w is the code weight (the number of "1") and λ_c is the cross correlation or the number of overlapping sequences.

There are two types of correlation functions, the auto-correlation function and the cross-correlation function. The auto-correlation function determines how well a code sequence is detected at an intended receiver in the presence of mutual interference. The cross-correlation represents the degree of mutual interference between two code sequences.

The auto-correlation property should be made as high possible to distinguish the signal in the presence of background noise. For a code sequence of $X = (x_1, x_2, \dots, x_N)$ it can be represented as:

$$\lambda_a = \sum_{i=1}^L x_i x_i \quad (3.1)$$

The cross-correlation property should be kept as low as possible to keep the Multiple Access Interference (MAI) as negligible as possible compared to the desired signal. For two code sequences $X = (x_1, x_2, \dots, x_N)$ and $Y = (y_1, y_2, \dots, y_N)$ it can be represented by:

$$\lambda_c = \sum_{i=1}^L x_i y_i \quad (3.2)$$

3.3 The Double Weight (DW) code

The DW code is a code proposed by Aljunid *et al* [20], for Spectral Amplitude Coding OCDMA systems. The DW code is constructed using a basic matrix construction and a mapping technique.

The DW code can be represented by using a $K \times N$ matrix. In the matrix K rows and N columns represent the number of users and the minimum code length respectively. A basic DW code is given by a 2×3 matrix as shown below:

$$H_{M=1} = \begin{bmatrix} 0 & 1 & 1 \\ 1 & 1 & 0 \end{bmatrix} \quad (3.3)$$

It can be noted out that $H_{M=1}$ has a chips combination sequence of 1,2,1 for the three columns. A chips combination sequence is defined by the summation of the values of the corresponding elements in every two rows (i.e 0+1, 1+1, 1+0). The purpose of the 1,2,1 combination is to maintain the cross correlation value of one; only one overlap between two chips will be allowed [20].

To increase the number of users a mapping technique is introduced:

$$H_{M=2} = - \left[\begin{array}{ccc|ccc} 0 & 0 & 0 & 0 & 1 & 1 \\ 0 & 0 & 0 & 1 & 1 & 0 \\ 0 & 1 & 1 & 0 & 0 & 0 \\ 1 & 1 & 0 & 0 & 0 & 0 \end{array} \right] = \begin{bmatrix} 0 & H_1 \\ H_1 & 0 \end{bmatrix} \quad (3.4)$$

Here, the basic matrix is repeated diagonally filling the empty spectrums with zeros '0' while maintaining the 1,2,1 combination. This mapping technique can be applied to increase the number of users from the basic number to any number of users.

The DW code has the following properties:

1. The code weight is two.
2. The cross-correlation is as most one.
3. The weighted chips are in pairs.
4. The chip combinations is maintained 1,2,1 for every three columns.

3.4 The Modified Double Weight (MDW) code

The MDW code is a member of the DW family, and has the same properties as the DW code. The main difference is that the weight is more than two (multiple of two) to increase the Signal to Noise Ratio (SNR) [48].

3.4.1 Basic Matrix Construction Technique

The MDW code is constructed using a basic matrix construction scheme [20]. The basic matrix construction is given in Figure 3.1.

$$\left[\begin{array}{c|c} [A] & [B] \\ \hline [C] & [D] \end{array} \right]$$

Figure 3.1: General Form for MDW basic matrix construction

Where:

1. $[A]$ consists of a $1 \times 3 \sum_{j=1}^{\frac{w}{2}-1} j$ matrix of zeros.
2. $[B]$ consists of a $1 \times 3n$ matrix of $[X_2]$ for every 3 column. (i.e. a $1 \times 3n$ matrix with n times repetition of $[X_2]$), where $n = \frac{w}{2}$.
3. $[C]$ is the basic code matrix for the next smaller weight, $w = 2(n-1)$.
4. $[D]$ is an $n \times n$ matrix of $[X_3]$ as shown in (3.5).

$$[D] = [X_3] = \begin{bmatrix} 000 & 000 & [X_3] \\ 000 & [X_3] & 000 \\ [X_3] & 000 & 000 \end{bmatrix} \quad (3.5)$$

Where

$$X_1 = [0 \ 0 \ 0] \quad (3.6)$$

$$X_2 = [0 \ 1 \ 1] \quad (3.7)$$

$$X_3 = [1 \ 1 \ 0] \quad (3.8)$$

There are two basic components constructing the basic matrix which are:

Basic Code Length:

$$N_B = 3 \sum_{m=1}^{\frac{w}{2}} m \quad (3.9)$$

Basic number of users:

$$K_B = \frac{w}{2} + 1 \quad (3.10)$$

Example (1):

An example of the MDW with the weight of six is given. For $w = 6$, from (3.9) the basic code length is:

$$N_B = 3 \sum_{j=1}^{\frac{w}{2}} j = 18 \quad (3.11)$$

and from (3.10), the basic number of users is:

$$K_B = \frac{w}{2} + 1 = 4 \quad (3.12)$$

Therefore, the basic matrix for MDW 6 consists of a 4 x 18 matrix. The element in each section depends on the value of n , for $w = 6$, $n=3$. The elements in the basic matrix for MDW at $w = 4$ are thus:

- a. [A] consists of a $1 \times 3 \sum_{j=1}^{\frac{w}{2}-1} j$ matrix of zeros, where $[A] = [[X_1], [X_1], [X_1]]$
 $= [0 \ 0 \ 0 \ 0 \ 0 \ 0 \ 0 \ 0 \ 0]$
- b. [B] consists of a $1 \times 3n$ matrix which is n repetition of $[X_2]$ or, in other words,
 $[B] = [[X_2], [X_2], [X_2]] = [0 \ 1 \ 1 \ 0 \ 1 \ 1 \ 0 \ 1 \ 1]$
- c. [C] consists of MDW basic matrix for the next smaller value of w (i.e. $w = 2(n-1) = 4$). The basic matrix for $w=4$ is,

After studying the matrix construction technique and the mapping technique, it can be observed that in order to get a specific codeword, it cannot be obtained without constructing the whole matrix in addition to using the mapping technique if the number of users is larger than the basic number. Due to this, it is necessary to establish an equation-based code construction technique to derive each codeword separately.

3.5 Equation-Based Code Construction

Two equations have been proposed for the DW code family construction.

3.5.1 The First Equation

By observing the representation of MDW in TABLE 3.2 and the mapping technique in TABLE 3.1, it can be seen that the mapping technique is simply images of the basic matrix repeated diagonally, so the basic matrix layout is concentrated on first, and then the mapping is taken into consideration later.

TABLE 3.2:
MDW OF WEIGHT SIX ($W = 6$) WITH ONES PATTERN.

| k^h | C_{18} | C_{17} | C_{16} | C_{15} | C_{14} | C_{13} | C_{12} | C_{11} | C_{10} | C_9 | C_8 | C_7 | C_6 | C_5 | C_4 | C_3 | C_2 | C_1 |
|-------|----------|----------|----------|----------|----------|----------|----------|----------|----------|-------|-------|-------|-------|-------|-------|-------|-------|-------|
| 1 | 0 | 0 | 0 | 0 | 0 | 0 | 0 | 0 | 0 | 0 | 1 | 1 | 0 | 1 | 1 | 0 | 1 | 1 |
| 2 | 0 | 0 | 0 | 0 | 1 | 1 | 0 | 1 | 1 | 0 | 0 | 0 | 0 | 0 | 0 | 1 | 1 | |
| 3 | 0 | 1 | 1 | 0 | 0 | 0 | 1 | 1 | 0 | 0 | 0 | 0 | 1 | 1 | 0 | 0 | 0 | 0 |
| 4 | 1 | 1 | 0 | 1 | 1 | 0 | 0 | 0 | 0 | 1 | 1 | 0 | 0 | 0 | 0 | 0 | 0 | 0 |

3.5.1.1 Pattern Observation

The number of ones is divided into two groups or patterns. The first pattern (grey pattern) consists of pairs of ones which are repeated on the same line consecutively separated by zeros. This first pattern has a total of w for the first user and decreases by 2 for every consecutive user. It reduces to zero for the last user (user number K_B).

The second pattern (black pattern) of pairs of ones has a diagonal pattern starting at the user number two and continuing to the last user. Additional diagonal patterns start at every consecutive user shifted from the previous pattern until the last user. The latter possesses a total number of ones from this second pattern, which is equals to w .

By applying the mapping technique the number of users is increased as shown in TABLE 3.1, the pattern structure being the same (only repeated).

3.5.1.2 Construction of the General Equation

Define the first right-hand column as column number one, and the first top row as row number one. The general formula can be represented as in (3.16).

$$MDW_{n,i} = \begin{cases} 1 & \text{if } \begin{cases} j = (n_1 - 1) + \left\lfloor \frac{(n_1 + 1)}{2} \right\rfloor \\ + \sum_{m=0}^{i \bmod K_B - 2} \left(\frac{3w}{2} - 3m \right) + \left\lfloor \frac{(i-1)}{K_B} \right\rfloor N_B & \text{for } n_1 = \{1, 2, \dots, w - 2((i-1) \bmod K_B)\} \\ j = 3((i-1) \bmod K_B) - 2 + \sum_{m=1}^{\left\lfloor \frac{(n_2 - 1)}{2} \right\rfloor} \left(\frac{3w}{2} - 3m \right) \\ + (n_2 - 1) \bmod 2 + 1 + \left\lfloor \frac{(i-1)}{K_B} \right\rfloor N_B & \text{for } n_2 = \{1, 2, \dots, 2((i-1) \bmod K_B)\} \end{cases} \\ 0 & \text{Otherwise} \end{cases} \quad (3.16)$$

Where *mod* represents modulo division, the symbol lower bounded $\lfloor x \rfloor$ denotes the integer portion of the real value of x , n_1 and n_2 represents the number of ones in each pattern described previously with $n_1 + n_2 = w$.

The first partial equation represents the plotting of the first pattern. The first two parts are used for plotting the pair of ones. The last two parts of the equation are used to shift the starting point of the pattern.

The second partial equation in the general formula plots the ones for the second pattern. Unlike the first pattern which comprises pairs of ones in sequences separated by zeros, the second pattern is more complex. The ones are grouped into diagonally shaped sets of pairs of ones.

For the user i with:

$$1 \leq i \leq K \quad (3.17)$$

Where K is the total number of users, and column j for the position of each chip:

$$1 \leq j \leq L \quad (3.18)$$

Where L is the maximum length given below:

$$L = \sum_{m=1}^{i \bmod K_B} \left(\frac{3(w-2(m-1))}{2} - \frac{1}{i \bmod K_B} \right) + \left\lfloor \frac{i}{K_B} \right\rfloor N_B \quad (3.19)$$

Example (2):

To fabricate user number 5 in TABLE 3.1, for a weight of four ($w=4$):

$$N_B = 3 \sum_{m=1}^2 m = 9 \quad (3.20)$$

$$K_B = 2 + 1 = 3 \quad (3.21)$$

To calculate the maximum length, use (3.19):

$$L = \sum_{m=1}^{5 \bmod 3} \left(\frac{3(4-2(m-1))}{2} - \frac{1}{5 \bmod 3} \right) + \left\lfloor \frac{5}{3} \right\rfloor 9 = 17 \quad (3.22)$$

From (3.16)

$$n_1 = \{1, 2\} \quad (3.23)$$

There are two ones in the first pattern.

$$n_2 = \{1, 2\} \quad (3.24)$$

There are two ones in the second pattern.

Substituting the value of n_1 and n_2 into (3.16), the values of j can be obtained by:

$$j = \{16, 17\} \text{ for } n_1 \quad (3.25)$$

$$j = \{11, 12\} \text{ for } n_2 \quad (3.26)$$

Inserting ones for each value of j , the codeword is obtained in Table 3.3:

TABLE 3.3:
THE FABRICATED CODEWORD NUMBER 5 USING (3.16)

| k^{th} | C_{17} | C_{16} | C_{15} | C_{14} | C_{13} | C_{12} | C_{11} | C_{10} | C_9 | C_8 | C_7 | C_6 | C_5 | C_4 | C_3 | C_2 | C_1 |
|----------|----------|----------|----------|----------|----------|----------|----------|----------|-------|-------|-------|-------|-------|-------|-------|-------|-------|
| 5 | 1 | 1 | 0 | 0 | 0 | 1 | 1 | 0 | 0 | 0 | 0 | 0 | 0 | 0 | 0 | 0 | 0 |

Here, it can be observed that the code obtained using the (3.16) in Table 3.3 is the same as codeword number 5 in TABLE 3.1.

3.5.2 The Second Equation

A second simplified equation based on the basic building blocks $[X_1]$, $[X_2]$ and $[X_3]$ is proposed for the code construction of the DW code family

3.5.2.1 Pattern Observation

By representing the MDW code construction shown in TABLE 3.4, with its basic building matrices $[X_1]$, $[X_2]$ and $[X_3]$, TABLE 3.5 is obtained.

TABLE 3.4:
MDW OF WEIGHT SIX ($W = 6$) WITH BASIC BLUIDING BLOCKS PATTERN.

| k^{th} | C_{18} | C_{17} | C_{16} | C_{15} | C_{14} | C_{13} | C_{12} | C_{11} | C_{10} | C_9 | C_8 | C_7 | C_6 | C_5 | C_4 | C_3 | C_2 | C_1 |
|----------|----------|----------|----------|----------|----------|----------|----------|----------|----------|-------|-------|-------|-------|-------|-------|-------|-------|-------|
| 1 | 0 | 0 | 0 | 0 | 0 | 0 | 0 | 0 | 0 | 0 | 1 | 1 | 0 | 1 | 1 | 0 | 1 | 1 |
| 2 | 0 | 0 | 0 | 0 | 1 | 1 | 0 | 1 | 1 | 0 | 0 | 0 | 0 | 0 | 0 | 1 | 1 | 0 |
| 3 | 0 | 1 | 1 | 0 | 0 | 0 | 1 | 1 | 0 | 0 | 0 | 0 | 1 | 1 | 0 | 0 | 0 | 0 |
| 4 | 1 | 1 | 0 | 1 | 1 | 0 | 0 | 0 | 0 | 1 | 1 | 0 | 0 | 0 | 0 | 0 | 0 | 0 |

TABLE 3.5:
MDW OF WEIGHT SIX ($W = 6$) WITH $[X_1]$, $[X_2]$ AND $[X_3]$

| k^{th} | 6 | 5 | 4 | 3 | 2 | 1 |
|----------|-------|-------|-------|-------|-------|-------|
| 1 | X_1 | X_1 | X_1 | X_2 | X_2 | X_2 |
| 2 | X_1 | X_2 | X_2 | X_1 | X_1 | X_3 |
| 3 | X_2 | X_1 | X_3 | X_1 | X_3 | X_1 |
| 4 | X_3 | X_3 | X_1 | X_3 | X_1 | X_1 |

By studying TABLE 3.5, two major patterns can be observed. The first pattern (grey pattern) consists of matrix $[X_2]$ which is repeated on the same line consecutively. This first pattern has a total number of $w/2$ from $[X_2]$ for the first user and decreases by one for every consecutive user. It reduces to zero for the last user (user number K_B).

The second pattern (black pattern) of $[X_3]$ has a diagonal pattern starting at the user number two and continuing to the last user. Additional diagonal patterns start at every consecutive user shifted from the previous pattern until the last user. The last user is purely constructed from second pattern (of $[X_3]$). The empty spaces are filled with matrix $[X_1]$ to complete the whole table

As in the first equation when mapping is applied, the whole basic matrix is repeated diagonally, the pattern remains unchanged. The only difference is the empty spaces are filled with $[X_1]$, instead of 1.

3.5.2.2 Construction of the General Formula

Define the first right-hand column as column number one, and the first top row as row number one. The general formula can be represented as in (3.27), where *mod* represents modulo division, the symbol lower bounded $\lfloor x \rfloor$ denotes the integer portion of the real value of x , n_1 and n_2 represents the number of $[X_3]$ and $[X_2]$ in each pattern respectively, with $n_1 + n_2 = w/2$.

$$MDW_{i,j} = \begin{cases} X_3 & \text{if } j = (i-1) \bmod K_B + (n-1) \frac{w}{2} \\ & - \sum_{m=1}^{n-1} m + \left\lceil \frac{(i-1)}{K_B} \right\rceil \frac{N_B}{3} \quad \text{for } n = \{1, 2, \dots, (i-1) \bmod K_B\} \\ X_2 & \text{if } j = \sum_{m=1}^{(i-1) \bmod K_B} (K_B - m) + n \\ & + \left\lceil \frac{(i-1)}{K_B} \right\rceil \frac{N_B}{3} \quad \text{for } n = \{1, 2, \dots, (K_B - 1) - (i-1) \bmod K_B\} \\ X_1 & \text{else} \end{cases} \quad (3.27)$$

In the general formula, there are two partial equations. The first plots the pattern for matrix $[X_3]$. The second partial equation represents the plotting of the second pattern for matrix $[X_2]$.

For the user i with:

$$1 \leq i \leq K \quad (3.28)$$

Where K is the total number of users, and column j for the position of each basic matrix:

$$1 \leq j \leq \left\lceil \frac{i}{K_B} \right\rceil N_B \quad (3.29)$$

Where $\lceil x \rceil$ is the ceiling function of x .

The code length is given with the same equation as in (3.19).

Example (3):

To fabricate user number 5, for a weight of four ($w=4$):

$$N_B = 3 \sum_{j=1}^2 j = 9 \quad (3.30)$$

$$K_B = 2 + 1 = 3 \quad (3.31)$$

To calculate the code length:

$$L = \sum_{m=1}^{5 \bmod 3} \left(\frac{3(W - 2(m - 1))}{2} - \frac{1}{5 \bmod 3} \right) + \left\lfloor \frac{5}{3} \right\rfloor 9 = 17 \quad (3.32)$$

Using equation (3.27), replace i with 4:

$$n_1 = \{1\} \quad (3.33)$$

There is one $[X_3]$ in the first pattern.

$$n_2 = \{1\} \quad (3.34)$$

There is one $[X_2]$ in the second pattern.

Substituting the value of n_1 and n_2 into (3.27), the values of j as follows are:

$$j = \{4\} \text{ for } n_1 \quad (3.35)$$

$$j = \{6\} \text{ for } n_2 \quad (3.36)$$

By inserting $[X_3]$ and $[X_2]$ in the positions determined by j , TABLE 3.6 is obtained.

TABLE 3.6:
THE FABRICATED CODEWORD NUMBER FIVE
USING (3.27) WITH $[X_1]$, $[X_2]$ AND $[X_3]$

| k^{th} | 6 | 5 | 4 | 3 | 2 | 1 |
|----------|-------|-------|-------|-------|-------|-------|
| MDW | X_2 | X_1 | X_3 | X_1 | X_1 | X_1 |

After transferring back to binary numbers, the desired codeword is obtained as in TABLE 3.7.

TABLE 3.7:
THE FABRICATED CODEWORD NUMBER FIVE USING (3.27) WITH CHIPS
REPRESENTATION

| k^n | C_{17} | C_{16} | C_{15} | C_{14} | C_{13} | C_{12} | C_{11} | C_{10} | C_9 | C_8 | C_7 | C_6 | C_5 | C_4 | C_3 | C_2 | C_1 |
|-------|----------|----------|----------|----------|----------|----------|----------|----------|-------|-------|-------|-------|-------|-------|-------|-------|-------|
| 5 | 1 | 1 | 0 | 0 | 0 | 1 | 1 | 0 | 0 | 0 | 0 | 0 | 0 | 0 | 0 | 0 | 0 |

Here, it can be observed that the code obtained using the (3.27) in TABLE 3.7 is the same as the codeword number 5 in TABLE 3.1. Column 18 has been deleted due to the code length equation (unused spectra).

3.6 Summary

In conclusion, the DW code family construction is studied in detail. The existing technique, builds the basic matrix, and a mapping technique is applied to increase the number of users. The disadvantage of this technique is that the whole code sequence set must be built to obtain a specific codeword, in addition to the fact that the inner matrices construction is complicated and time consuming. A new code construction technique for the DW code family has been proposed. This new technique is purely based on mathematical equations. Two equations have been proposed, the first is based on the distributions of ones '1' in each codeword and the second is based on the pattern of the basic building blocks of the basic matrix ($[X_1], [X_2]$ and $[X_3]$). Both equations are simple, accurate, precise and, most importantly, can obtain any specific codeword for any weight for any number of users without the need to construct the whole set of code sequences. Another major advantage of an equation based construction technique is that it can be used in mathematical analysis (comparison between codes e.g. code length), where the old construction technique cannot be used. An equation for the exact code length has also been proposed to preset the number of wavelengths need for the system.

CHAPTER FOUR

PERFORMANCE ANALYSIS ON THE DETECTION SCHEME

4.1 Introduction

This chapter discusses the detection schemes for the double weight DW code family. This chapter begins with an overview of Multiple Access Interference effects, noise definitions and OCDMA detection schemes. The performance of the DW code family is then evaluated using the complementary detection technique. The mapping technique is applied to increase the number of users, but at a cost of an unfixed cross-correlation property. A hybrid Wavelength Division Multiplexing/Spectral Amplitude Coding (WDM/SAC) scheme is applied to overcome this change in the cross-correlation property. A mathematical method to reduce the number of Fiber Bragg Gratings (FBG) and to minimize the Phase Induced Intensity Noise is proposed for the DW code family. A simulation for all the three systems for the MDW code of weight four ($w=4$) is implemented using the Virtual Photonics Instrument (VPI).

4.2 Multiple Access Interference (MAI)

The main target of an Optical CDMA system is to extract the desired user data in the presence of other users' data. The MAI represents a dominant source of noise in Direct Spreading Optical CDMA systems [12-13], where the desired user's data is interfered with. Spectral Amplitude Coding systems [16-17], have been proposed to cancel the MAI by using appropriate detection schemes.

The MAI is present in SAC systems due to the fact that different users occupy the same spectra (overlapping chips) as the desired user, which corrupt the data intended for that specific user unless correctly detected.

The presence of overlapping spectra causes another type of noise known as Phase Induced Intensity Noise (PIIN). PIIN results from the phase incoherence of the overlapping signals on the same spectra causing fluctuations in the total signal intensity. It can be noted that although the PIIN is caused by MAI, the reduction of MAI at the electrical layer will not eliminate the PIIN. This is because this will only filter out the unwanted data, not the intensity noise that already happens at the photodetector. An effective way of reducing the PIIN is by reducing the interference at the optical layer itself. This can be achieved by keeping the in-phase cross-correlation ideal ($\lambda = 1$).

4.3 Noise Estimation

Any signal that is present with the intended signal is considered as noise. In other words, any signal that interferes with the desired signal in any way whatsoever is regarded as noise. Noise can be divided into two categories. The first is Intrinsic Noise which arises due to the physical aspects of the system design particularly in the optoelectronic and electronic devices used to construct the receiver. Examples of intrinsic noise are PIIN, thermal noise and shot noise. The second is Coupled Noise arising from interactions between the receiver circuitry and the surrounding environment. Atmospheric disturbances, nearby power supplies, and fast switching logic circuitry are some examples of coupled noise.

4.3.1 Phase Induced Intensity Noise

Phase Induced Intensity Noise (PIIN) is caused when incoherent light fields are mixed and incident upon a photodetector, the phase noise of the fields generates an intensity noise. For the mixing of two uncorrelated identically polarized light fields, assuming that they have negligible self-intensity noise, having the same spectrum and intensity, and that the spectral width is very much larger than the maximum electrical bandwidth, the photocurrent variance due to PIIN is given by [49].

$$\langle I_{PIIN}^2 \rangle = I \tau_c B \quad (4.1)$$

Where τ_c is the coherence time of the source, I is the average photocurrent and B is the noise equivalent electrical bandwidth of the receiver [18].

Since PIIN cannot be canceled at the electrical detection level, the only way to reduce the PIIN is to keep the cross-correlation at its lowest possible value ($\lambda = 1$).

4.3.2 Shot Noise

Shot noise in electronic circuits is strongly related to the random nature of charges that pass a certain point in a circuit. The statistics that describe the charge crossing determines the noise characteristics. If the charge crossing is periodic and predictable, then no noise is generated, but if the charge crossing is random and independent of the number of carriers proceeding or following, then noise can be represented with Poisson distribution. A Gaussian distribution can be used when the number of events per time unit is large [51].

Shot noise can be represented by:

$$\langle I_{shot}^2 \rangle = 2eIB \quad (4.2)$$

Where e is the electronic charge, B is the noise equivalent electric bandwidth.

4.3.3 Thermal Noise

Thermal noise is due to induced random fluctuations in the charge carriers in a resistance. Since resistors are present in the photodetector, thermal noise is present in photodetectors [51].

Thermal noise can be expressed by:

$$\langle I_{Thermal}^2 \rangle = \frac{4K_bTB}{R_L} \quad (4.3)$$

Where T is the absolute temperature, K_b is the Boltzmann's constant, B is the noise-equivalent electrical bandwidth of the receiver and R_L is the receiver load resistance.

4.4 Optical CDMA Systems

Optical CDMA systems can be divided into two major categories. The first is coherent systems, where knowledge of the phase and amplitude is needed in order to achieve successful detection. Bipolar codes are used in coherent systems [28-29]. The second is incoherent systems, where the performance of the system depends mainly on the amplitude. Unipolar codes are used mainly in incoherent systems [19-20], although bipolar codes can also be obtained by sending complementary spectrally encoded signals in SAC systems [17-18].

Coherent systems need more expensive and complex hardware than incoherent systems for the purpose of phase synchronization.

This research concentrates on incoherent SAC OCDMA systems as they show better results than other incoherent systems [16]. Coherent systems have been excluded due to their complexity and high cost of equipment.

In incoherent SAC systems each user is assigned with a unique signature sequence (codeword) depending on the spectral amplitude. The MAI can be totally canceled in SAC systems by using the balanced detection technique [16].

4.5 Spectral Amplitude Coding Detection Schemes

Spectral Amplitude Coding (SAC) systems use complementary detection technique to recover the original signal. Complementary detection can successfully retrieve desired signals only for codes which have fixed cross-correlation. An example of a complementary detection system is shown in Figure 4.1.

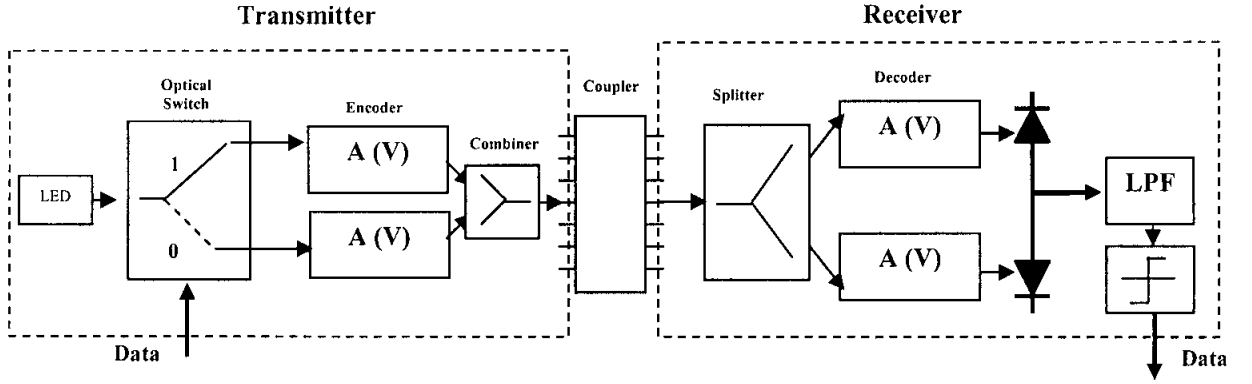


Figure 4.1: Complementary Detection Scheme

The system shown in Figure 4.1 is for the m -sequence and Hadamard codes [17-18], where the transmitter sends a pulse with the spectral distribution of $A(v)$ to represent data '1', and a pulse with a complementary spectral distribution of $\bar{A}(v)$ to represent data '0'. All the signals are mixed and coupled together and sent to all receivers. At the receiver the signal is split into two, and decoded by two complementary decoders. After the balanced detection the signal is passed to a low pass filter and threshold decision and after that the original signal can be recovered.

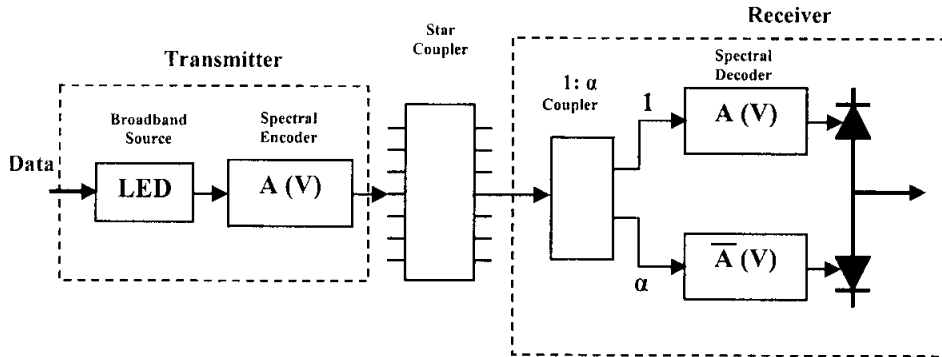


Figure 4.2: SAC System for Non-Complementary Codes

The system shown in Figure 4.2 is for unipolar codes, where a pulse with a spectral distribution of $A(v)$ is sent to represent data '1' and nothing is sent to represent data '0' [13-17]. At the receiver, the signal is split into two by 1: α splitter. If the code is $a(L, w, \lambda)$, then the MAI for $(k-1)$ user at the first photodetector is $\lambda(k-1)$ and the MAI

at the second photodetector is $\alpha(w - \lambda)(k - 1)$. When $\alpha = (w - \lambda)/\lambda$, the MAI on both receivers is equal and can be canceled by balanced detection.

4.6 Double Weight Code Family Detection

Three detection schemes are analyzed for DW code family detection, the Complementary detection scheme, the hybrid Wavelength Division Multiplexing/Spectral Amplitude Coding (WDM/SAC) scheme and the reduced set of Fiber Bragg Gratings WDM/SAC scheme.

4.6.1 Complementary Detection Scheme

The basic matrix of the DW code family can be detected by the complementary detection scheme, due to that fact that all code sequences in the basic matrix all correlate ideally together ($\lambda = 1$). Figure 4.3 shows, the complementary SAC decoder with Fiber Bragg Gratings (FBG).

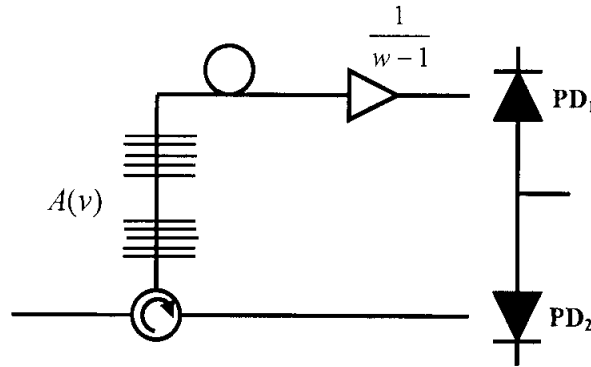


Figure 4.3: Complementary SAC decoder using FBGs.

4.6.1.1 Performance Analysis

The variance of the photodiode current is given by:

$$\langle i^2 \rangle = 2eIB + I^2 B \tau_c + \frac{4K_b T_n B}{R_L} \quad (4.4)$$

Where e is the Electron's charge, I is the Average photocurrent, B is the Noise equivalent electrical Bandwidth of the receiver, τ_c is the Coherence time of the source, K_b is the

Boltzmann's Constant, T_n is the Absolute receiver noise temperature, R_L is the Receiver load resistor.

In the equation above the first term represents the shot noise, the second is PIIN noise and the third term is the thermal noise.

To calculate the coherence time τ_c , assume the single sideband Power Spectral Density (PSD) is $G(\nu)$, τ_c can be given by [18]:

$$\tau_c = \frac{\int_0^\infty G^2(\nu) d\nu}{\left[\int_0^\infty G(\nu) d\nu \right]^2} \quad (4.5)$$

The code properties of the DW code family are:

$$\sum_{i=1}^L C_k(i) C_l(i) = \begin{cases} w, & \text{For } k=l \\ 1, & \text{For } k \neq l \end{cases} \quad (4.6)$$

and

$$\sum_{i=1}^L C_k(i) \bar{C}_l(i) = \begin{cases} 0, & \text{For } k=l \\ w-1, & \text{For } k \neq l \end{cases} \quad (4.7)$$

To analyze the DW code family using the system in Figure 4.3, assume [46]:

1. Each light source is ideally unpolarized and its spectrum is flat over the bandwidth $[\nu_0 - \Delta\nu/2, \nu_0 + \Delta\nu/2]$ where ν_0 is the central optical frequency and $\Delta\nu$ is the optical source bandwidth in Hertz.
2. Each power spectral component has identical spectral width.
3. Each user has equal power at the receiver.
4. Each bit stream from each user is synchronized.

Using the assumptions above, the system can be easily analyzed using a Gaussian approximation. The PSD can be represented by:

$$r(v) = \frac{P_{sr}}{\Delta V} \sum_{k=1}^K d_k \sum_{i=1}^L c_k(i) \left\{ u \left[v - v_o - \frac{\Delta v}{2L} (-L + 2i - 2) \right] - u \left[v - v_o - \frac{\Delta v}{2L} (-L + 2i) \right] \right\} \quad (4.8)$$

where P_{sr} is the effective power of a broadband source at the receiver, K is the active number of users, L is the DW code length, d_k is the data bit of the k th user that is “1” or “0”, and $u(v)$ is the unit step function expressed as :-

$$u(v) = \begin{cases} 1, & v \geq 0 \\ 0, & v < 0 \end{cases} \quad (4.9)$$

The PSD of PD₁ and PD₂ is given by:

$$G_1(v) = \frac{P_{sr}}{\Delta v} \sum_{k=1}^K d_k \sum_{i=1}^L C_k(i) \bar{C}_l(i) \left\{ u \left[v - v_0 - \frac{\Delta v}{2L} (-L + 2i - 2) \right] - u \left[v - v_0 - \frac{\Delta v}{2L} (-L + 2i) \right] \right\} \quad (4.10)$$

$$G_2(v) = \frac{P_{sr}}{\Delta v} \sum_{k=1}^K d_k \sum_{i=1}^L C_k(i) C_l(i) \left\{ u \left[v - v_0 - \frac{\Delta v}{2L} (-L + 2i - 2) \right] - u \left[v - v_0 - \frac{\Delta v}{2L} (-L + 2i) \right] \right\} \quad (4.11)$$

Then, integrating the power spectral density,

$$\int_0^\infty G_1(v) dv = \frac{P_{sr}}{L} \sum_{k=1}^K d_k \quad (4.12)$$

and

$$\int_0^\infty G_2(v) dv = \frac{P_{sr}}{L} w dl + \frac{P_{sr}}{L} \sum_{k=1}^K d_k \quad (4.13)$$

To find $G_1^2(\nu)$ and $G_2^2(\nu)$, examine the example of the PSD shown in Figure 4.4 for the superimposed signal $r(\nu)$. Where $A(i)$ represents the amplitude of the spectral slot number i with a width of $\Delta\nu/L$.

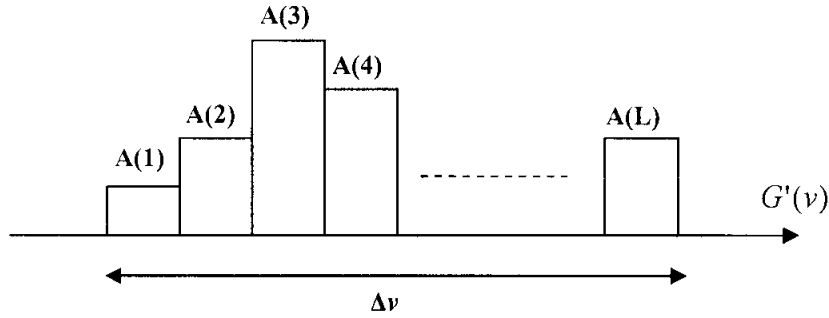


Figure 4.4: The PSD of the Received Signal $r(\nu)$.

The integral of $G^2(\nu)$ can be expressed as:

$$\int_0^{\infty} G^2(\nu) d\nu = \frac{\Delta\nu}{L} \sum_{i=1}^N A^2(i) \quad (4.14)$$

Therefore,

$$\int_0^{\infty} G_1^2(\nu) d\nu = \frac{1}{(w-1)^2} \frac{P_{sr}^2}{L\Delta\nu} \sum_{i=1}^L \left\{ \bar{C}_l(i) \cdot \left[\sum_{k=1}^K d_k C_k(i) \right] \cdot \left[\sum_{m=1}^K d_m C_m(i) \right] \right\} \quad (4.15)$$

and

$$\int_0^{\infty} G_2^2(\nu) d\nu = \frac{P_{sr}^2}{L\Delta\nu} \sum_{i=1}^L \left\{ C_l(i) \cdot \left[\sum_{k=1}^K d_k C_k(i) \right] \cdot \left[\sum_{m=1}^K d_m C_m(i) \right] \right\} \quad (4.16)$$

In the above equations, d_k is the data bit of the k_{th} user that carries the value of either “1” or “0”. Consequently, the photocurrent I can be expressed as:

$$I = I_2 - I_1 = \Re \int_0^{\infty} G_2(\nu) d\nu - \Re \int_0^{\infty} G_1(\nu) d\nu \quad (4.17)$$

Substitute (4.12) and (4.13) in Equation (4.17),

$$\text{Photocurrent, } I = \Re \left[\frac{P_{sr}}{L} \right] \cdot \left[w + \sum_{k=1}^K d_k - \sum_{k=1}^K d_k \right] \quad (4.18)$$

$$I = \Re \left[\frac{P_{sr} w}{L} \right] \quad (4.19)$$

Where \Re is the responsivity of the photodetectors given by:

$$\Re = \frac{\eta e}{h \nu_c} \quad (4.20)$$

Where

- η is the quantum efficiency
- e is the electron's charge
- h is the Planck's constant
- ν_c is the central frequency of the original broad-band optical pulse

Since the noise in each photodetector (PD₁ and PD₂) is independent the total noise can be represented by:

$$\langle I^2 \rangle = \langle I_{sh}^2 \rangle + \langle I_{piin}^2 \rangle + \langle I_{th}^2 \rangle \quad (4.21)$$

$$\langle I^2 \rangle = 2eB(I_1 + I_2) + BI_1^2 \tau_{c1} + BI_2^2 \tau_{c2} + \frac{4K_b T_n B}{R_L} \quad (4.22)$$

Therefore,

$$\begin{aligned} \langle I^2 \rangle = 2eB \Re \left[\int_0^\infty G_1(\nu) d\nu + \int_0^\infty G_2(\nu) d\nu \right] \\ + B \Re^2 \int_0^\infty G_1^2(\nu) d\nu + B \Re^2 \int_0^\infty G_2^2(\nu) d\nu + \frac{4K_b T_n B}{R_L} \end{aligned} \quad (4.23)$$

From (4.15) and (4.16), when all the users are transmitting bit “1” using the average value as $\sum_{k=1}^K c_k(i) \approx \frac{Kw}{L}$ and the noise power can be written as :-

$$\begin{aligned} \langle I^2 \rangle = & 2eB\Re \left[\frac{P_{sr}}{L} ((K-1) + w + (K-1)) \right] \\ & + B\Re^2 \left[\frac{P_{sr}Kw}{\Delta v L^2} \left(\left(\frac{K-1}{w-1} \right) + w + (K-1) \right) \right] + \frac{4K_b T_n B}{R_L} \end{aligned} \quad (4.24)$$

The probability of sending bit ‘1’ is $\frac{1}{2}$ then:

$$\begin{aligned} \langle I^2 \rangle = & \frac{P_{sr} eB \Re}{L} [w + 2(K-1)] \\ & + \frac{P_{sr}^2 B \Re^2 Kw}{2 \Delta v L^2} \left[\frac{K-1}{w-1} + w + K-1 \right] + \frac{4K_b T_n B}{R_L} \end{aligned} \quad (4.25)$$

The Signal to Noise Ratio can be expressed by:

$$SNR = \frac{(I_2 - I_1)^2}{\langle I^2 \rangle} \quad (4.26)$$

$$SNR = \frac{\frac{\Re^2 P_{sr}^2 w^2}{L^2}}{\frac{P_{sr} eB \Re}{L} [w + 2(K-1)] + \frac{P_{sr}^2 B \Re^2 Kw}{2 \Delta v L^2} \left[\frac{K-1}{w-1} + w + K-1 \right] + \frac{4K_b T_n B}{R_L}} \quad (4.27)$$

Equation (4.27) is the general equation used to calculate the signal to noise ratio for the DW code families. Using Gaussian approximation, the Bit Error Rate (BER) can be expressed as:

$$BER = P_e = \frac{1}{2} \operatorname{erfc} \left(\sqrt{\frac{SNR}{8}} \right) \quad (4.28)$$

4.6.2 Hybrid Wavelength Division Multiplexing/Spectral Amplitude Coding

In order to increase the number of users in the DW code family, a mapping technique must be applied. The Mapping technique functions by diagonally repeating the basic matrix, and filling the empty spaces with zeros. This number of user increment leads to an unfixed cross-correlation due to the fact that the cross-correlation is fixed to one between the code sequences of any of the repeated basic matrices and zero with any other code sequence.

The complementary detection technique, as previously stated, can successfully cancel all the MAI only if all the code sequences have a fixed cross-correlation with each other. A hybrid Wavelength Division Multiplexing/Spectral Amplitude Coding (WDM/SAC) Optical CDMA system is given in [52], where balanced detection can be achieved even if the cross-correlation is not fixed to a specific number.

To analyze the DW code family with the hybrid WDM/SAC, examine the MDW code of weight four ($w = 4$) with two mappings ($N = 2$) the code sequences are shown in TABLE 4.1

TABLE 4.1:
MDW OF WEIGHT FOUR ($W = 4$) WITH MAPPING.

| k^{th} | C_{18} | C_{17} | C_{16} | C_{15} | C_{14} | C_{13} | C_{12} | C_{11} | C_{10} | C_9 | C_8 | C_7 | C_6 | C_5 | C_4 | C_3 | C_2 | C_1 |
|----------|----------|----------|----------|----------|----------|----------|----------|----------|----------|-------|-------|-------|-------|-------|-------|-------|-------|-------|
| 1 | 0 | 0 | 0 | 0 | 0 | 0 | 0 | 0 | 0 | 0 | 0 | 0 | 0 | 1 | 1 | 0 | 1 | 1 |
| 2 | 0 | 0 | 0 | 0 | 0 | 0 | 0 | 0 | 0 | 0 | 1 | 1 | 0 | 0 | 0 | 1 | 1 | 0 |
| 3 | 0 | 0 | 0 | 0 | 0 | 0 | 0 | 0 | 0 | 1 | 1 | 0 | 1 | 1 | 0 | 0 | 0 | 0 |
| 4 | 0 | 0 | 0 | 0 | 1 | 1 | 0 | 1 | 1 | 0 | 0 | 0 | 0 | 0 | 0 | 0 | 0 | 0 |
| 5 | 0 | 1 | 1 | 0 | 0 | 0 | 1 | 1 | 0 | 0 | 0 | 0 | 0 | 0 | 0 | 0 | 0 | 0 |
| 6 | 1 | 1 | 0 | 1 | 1 | 0 | 0 | 0 | 0 | 0 | 0 | 0 | 0 | 0 | 0 | 0 | 0 | 0 |

By observing TABLE 4.1, it can be seen that the cross-correlation between code sequences within the same basic matrix (grey matrices) is fixed to '1' and with other code sequences is '0'.

Figure 4.5 shows the hybrid WDM/SAC encoder and decoder design for user number 1 from TABLE 4.1.

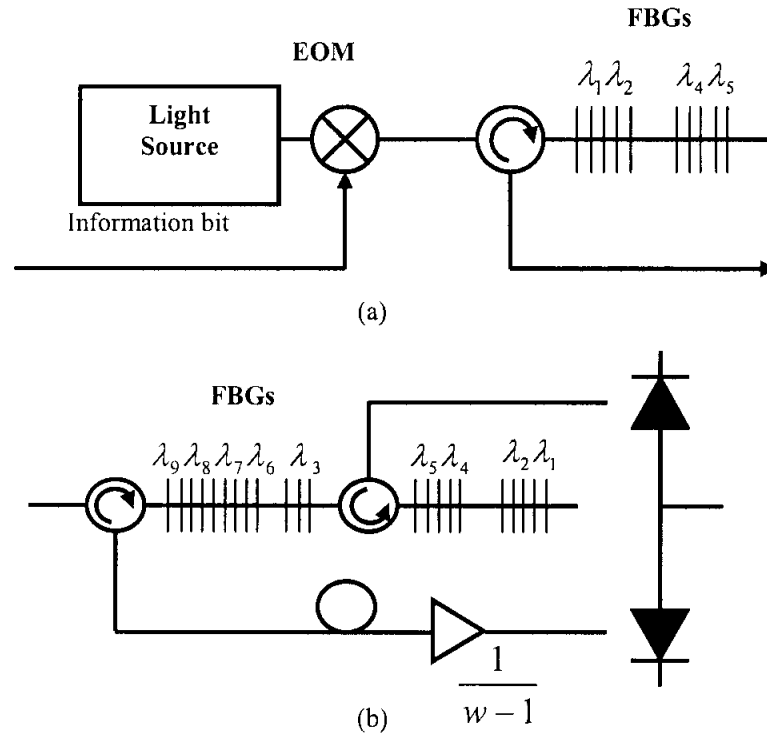


Figure 4.5: Structure of (a) Encoder and (b) Decoder for user number 1 using MDW with mapping using FBGs.

At the encoder, the information bit is used as ON-OFF keying to the incoherent broadband optical source. The signal is then directed to the FBGs, where each chip of user number 1 has been attributed with a specific wavelength. The placement of the FBGs depends upon the chip value. Only the chip '1' is represented.

The decoder design has the same concept as the complementary technique, where the received signal is passed through two FBGs, and the result circulated to photodetectors [52]. The main principle behind the decoder design is only codes that correlate with intended receiver are circulated to both photodetectors. Codes that do not correlate pass without getting detected.

4.6.2.1 Performance Analysis

Assuming there is N repetition of the basic matrix, the correlation function for each photodetector is given by:

$$R_{D1} = \begin{cases} w, & \text{for } k=l \\ 1, & \text{for } \left\lfloor \frac{l-1}{K_B} \right\rfloor K_B + 1 \leq k \leq \left\lfloor \frac{l-1}{K_B} \right\rfloor K_B + K_B \text{ \& } k \neq l \\ 0, & \text{else} \end{cases} \quad (4.29)$$

and

$$R_{D2} = \begin{cases} 0, & \text{for } k=l \\ w-1, & \text{for } \left\lfloor \frac{l-1}{K_B} \right\rfloor K_B + 1 \leq k \leq \left\lfloor \frac{l-1}{K_B} \right\rfloor K_B + K_B \text{ \& } k \neq l \\ 0, & \text{else} \end{cases} \quad (4.30)$$

Thus MAI can be canceled by:

$$R_{D1} - \frac{R_{D2}}{W-1} = \begin{cases} w & k=l \\ 0 & \text{else} \end{cases} \quad (4.31)$$

The photodetector current can be calculated by integrating:

$$\int_0^\infty R_{D1}(v) dv = \frac{P_{sr}}{L} \sum_{k=1}^K d_k \quad (4.32)$$

and

$$\int_0^\infty R_{D2}(v) dv = \frac{P_{sr}}{L} w dl + \frac{P_{sr}}{L} \sum_{k=1}^K d_k \quad (4.33)$$

The photocurrent can be expressed as:

$$I = \Re \int_0^{\infty} R_{D1}(\nu) d\nu - \Re \int_0^{\infty} R_{D2}(\nu) d\nu \quad (4.34)$$

$$I = \Re \left[\frac{P_{sr} w}{L} \right] \quad (4.35)$$

The SNR is calculated using the following equation:

$$SNR = \frac{\langle I^2 \rangle}{\langle I_{piin}^2 \rangle + \langle I_{sh}^2 \rangle + \langle I_{th}^2 \rangle} \quad (4.36)$$

To calculate the Phase Induced Intensity Noise (PIIN), Shot Noise and Thermal Noise, the same procedure is used as in [46] to give more accurate results:

$$\langle I_{piin}^2 \rangle = \frac{P_{sr}^2 B \Re^2 w K}{2 \Delta \nu L^2 N} \left[\frac{(K-1)/N}{w-1} + w + (K-1)/N \right] \quad (4.37)$$

The shot noise:

$$\langle I_{sh}^2 \rangle = \frac{P_{sr} e B \Re}{L} [w + 2(K-1)/N] \quad (4.38)$$

The thermal noise:

$$\langle I_{th}^2 \rangle = \frac{4 K_b T_n B}{R_b} \quad (4.39)$$

The BER can be calculated by:

$$BER = \frac{1}{2} \operatorname{erfc} \left(\sqrt{\frac{SNR}{8}} \right) \quad (4.40)$$

4.6.3 A Reduced Number of Fiber Bragg Gratings Approach

By studying the hybrid WDM/SAC system for the DW code family, it can be observed that for each user that correlates with the desired signal only one wavelength is circulated to the first photodetector. So it is possible to circulate one wavelength instead of $w-1$ from each user which correlates with intended user to the second photodetector, the MAI can be totally canceled and the number of FBGs can be reduced. A mathematical approach is proposed to select the wavelengths that can achieve both a reduction in the number of FBGs and minimization in the PIIN.

The proposed decoder design is shown in Figure 4.6 where are minimum number of FBGs is used.

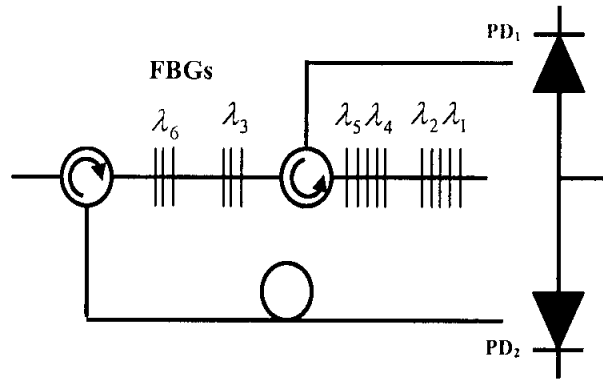


Figure 4.6: Structure of proposed reduced set of FBGs decoder for user number 1 using MDW ($w=4$) with mapping.

The first set of FBGs that circulates to the first photodetector has the same positioning as in Figure 4.5(a), the wavelength selection can be chosen using the first construction equation in chapter three. A reduction to $w/2$ of number of FBGs can be achieved for the second set of FBGs, by circulating only one wavelength for each user that correlate with intended receiver signal to the second photodetector. This is achieved by placing one FBG for each user. In order minimize the PIIN on the second photodetector, the wavelengths that do not correlate to any other chips are chosen.

There are many ways of selecting the wavelengths for the FBGs for the second set. One way is to select wavelength positions using (4.41). The equation given in (4.41) has the same pattern as the first construction equation in chapter three.

$$FBG_{i,j} = \begin{cases} j = 3n_1 + \sum_{m=0}^{i \bmod K_B - 2} \left(\frac{3w}{2} - 3m \right) + \left\lfloor \frac{(i-1)}{K_B} \right\rfloor N_B & \text{for } n_1 = \{1, 2, \dots, (w - 2((i-1) \bmod K_B))/2\} \\ j = 3((i-1) \bmod K_B) - 2 + \sum_{m=1}^{n_2-1} \left(\frac{3w}{2} - 3m \right) + \left\lfloor \frac{(i-1)}{K_B} \right\rfloor N_B & \text{for } n_2 = \{1, 2, \dots, ((i-1) \bmod K_B)\} \end{cases} \quad (4.41)$$

Example (1):

For user is number 1 from TABLE 4.1. To design the receiver, the first set of FBGs can be chosen using the first equation based construction method given in chapter three. To find the position of the FBGs in the second set:

First calculate n_1 and n_2 :

$$n_1 = \{1\} \quad (4.42)$$

$$n_2 = \{1\} \quad (4.43)$$

By substituting the values of n_1 and n_2 into (4.41), obtain the positions of the wavelength needed:

$$j = \{9\} \quad (4.44)$$

$$j = \{1\} \quad (4.45)$$

So by placing two FBGs at wavelength number one and wavelength number nine, only these two wavelengths will be circulated to the second photodetector. Due the fact that chips that correlate are not detected at the second photodetector, the PIIN is minimized at the second photodetector.

4.6.3.1 Performance Analysis

The correlation functions for each photodetector for Figure 4.3 are given by:

$$R_{D1} = \begin{cases} w, & \text{for } k=l \\ 1, & \text{for } \left\lfloor \frac{l-1}{K_B} \right\rfloor K_B + 1 \leq k \leq \left\lfloor \frac{l-1}{K_B} \right\rfloor K_B + K_B \text{ \& } k \neq l \\ 0, & \text{else} \end{cases} \quad (4.46)$$

and

$$R_{D2} = \begin{cases} 0, & \text{for } k=l \\ 1, & \text{for } \left\lfloor \frac{l-1}{K_B} \right\rfloor K_B + 1 \leq k \leq \left\lfloor \frac{l-1}{K_B} \right\rfloor K_B + K_B \text{ \& } k \neq l \\ 0, & \text{else} \end{cases} \quad (4.47)$$

Thus MAI can be canceled by:

$$R_{D1} - R_{D2} = \begin{cases} w & k=l \\ 0 & \text{else} \end{cases} \quad (4.48)$$

The PIIN can be calculated by:

$$\langle I_{pn}^2 \rangle = \frac{P_{sr}^2 B \mathfrak{R}^2}{2 \Delta \nu L^2} \frac{w K}{N} [w + (K-1)/N] \quad (4.49)$$

The shot noise can be given by:

$$\langle I_{sh}^2 \rangle = \frac{P_{sr} e B \mathfrak{R}}{L} [w + 2(K-1)/N] \quad (4.50)$$

By using (4.36) to obtain the SNR, the BER can be calculated by:

$$BER = \frac{1}{2} \operatorname{erfc} \left(\sqrt{\frac{SNR}{8}} \right) \tag{4.51}$$

4.7 Simulation Setup

A design for a SAC Optical CDMA system using the MDW code ($w=4$) with four users is implemented using the Virtual Photonics Instrument (VPI) version 7.1. TABLE 4.2 shows the code sequence for the each user.

TABLE 4.2:
CODE SEQUENCES FOR EACH USER IN THE SIMULATION

| k^h | C_{14} | C_{13} | C_{12} | C_{11} | C_{10} | C_9 | C_8 | C_7 | C_6 | C_5 | C_4 | C_3 | C_2 | C_1 |
|-------|----------|----------|----------|----------|----------|-------|-------|-------|-------|-------|-------|-------|-------|-------|
| 1 | 0 | 0 | 0 | 0 | 0 | 0 | 0 | 0 | 0 | 1 | 1 | 0 | 1 | 1 |
| 2 | 0 | 0 | 0 | 0 | 0 | 0 | 1 | 1 | 0 | 0 | 0 | 1 | 1 | 0 |
| 3 | 0 | 0 | 0 | 0 | 0 | 1 | 1 | 0 | 1 | 1 | 0 | 0 | 0 | 0 |
| 4 | 1 | 1 | 0 | 1 | 1 | 0 | 0 | 0 | 0 | 0 | 0 | 0 | 0 | 0 |

The system parameters are as follows; the wavelength used is 1550 μm , the frequency spacing is 100 MHz, the fiber attenuation is $0.2e^{-3}$ dB/km, the fiber dispersion is $16e^{-6}$ s/m², the modulator extinction is 30 dB, the laser power is $1e^{-3}$ W and the data rates used are 2.5 Gbps and 10 Gbps for distances from 1km to 100km. The simulation is kept as real as possible by activating all the attenuation parameters such as insertion loss and nonlinearities.

The schematic block design of the MDW code transmitter is given in Figure 4.7. The transmitter is externally modulated to support high data rates.

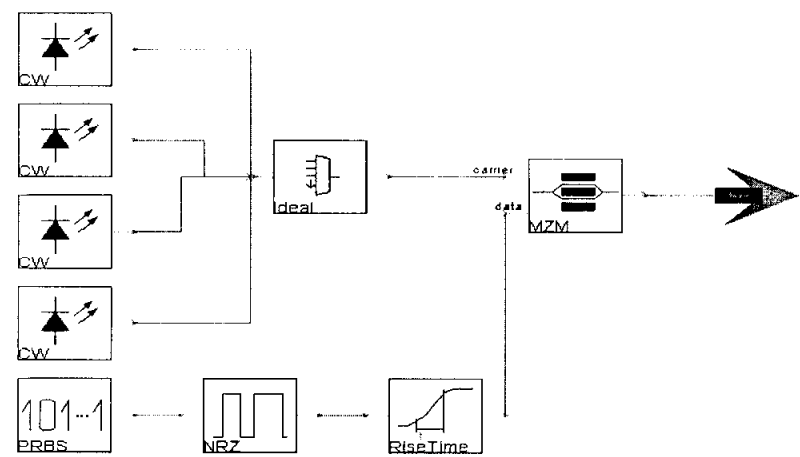


Figure 4.7: Transmitter Design for MDW code ($w=4$) system

Figure 4.8 shows the complementary SAC receiver, where the signal mainly is split into two. The first photodetector detect the signal with a spectral distribution of $A(v)$, and the second photodetector detects the complementary spectral distribution $\bar{A}(v)$.

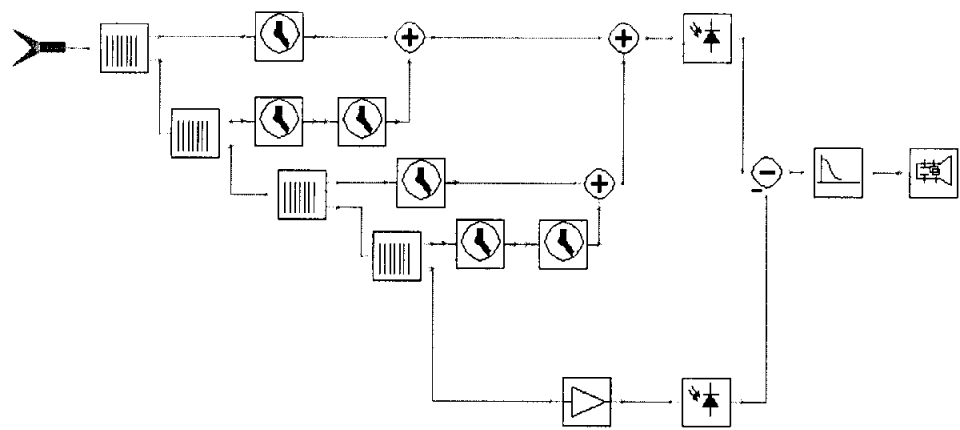


Figure 4.8: Receiver Design for Complementary SAC system

Figure 4.9 shows the hybrid WDM/SAC receiver. The received signal is split into two. Pulses with spectral distribution $A(\nu)$ are directed to the upper photodetector. Other pulses that correlate with the desired users are directed to the lower photodetector. Signals that do not correlate with intended receiver pass without getting detected.

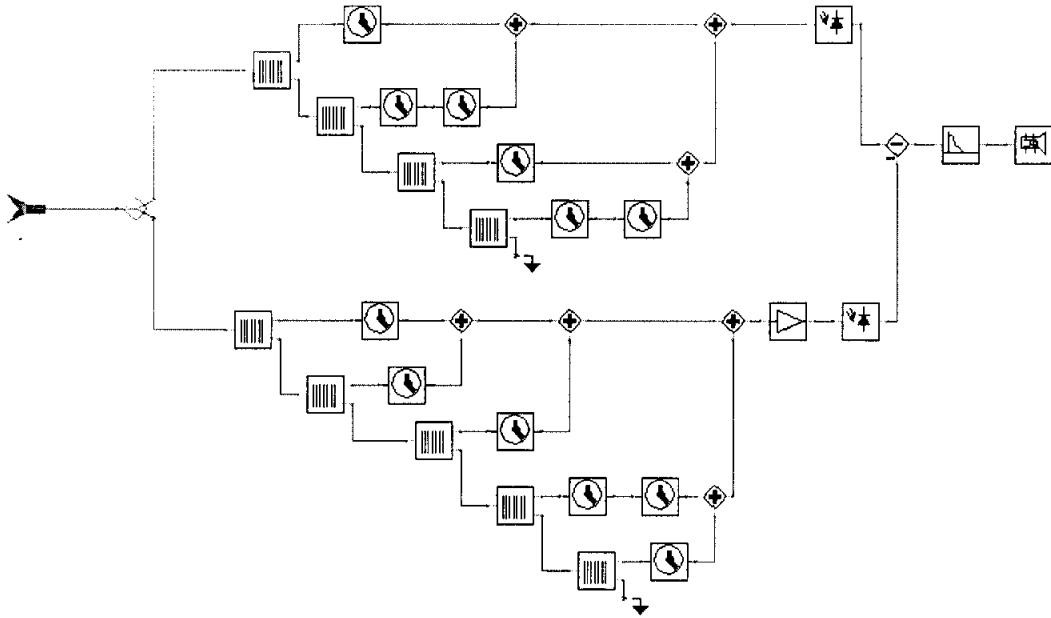


Figure 4.9: Receiver Design for Hybrid WDM/SAC system using FBGs

Figure 4.10 shows the receiver design for the reduced set of FBGs for Hybrid WDM/SAC detection scheme.

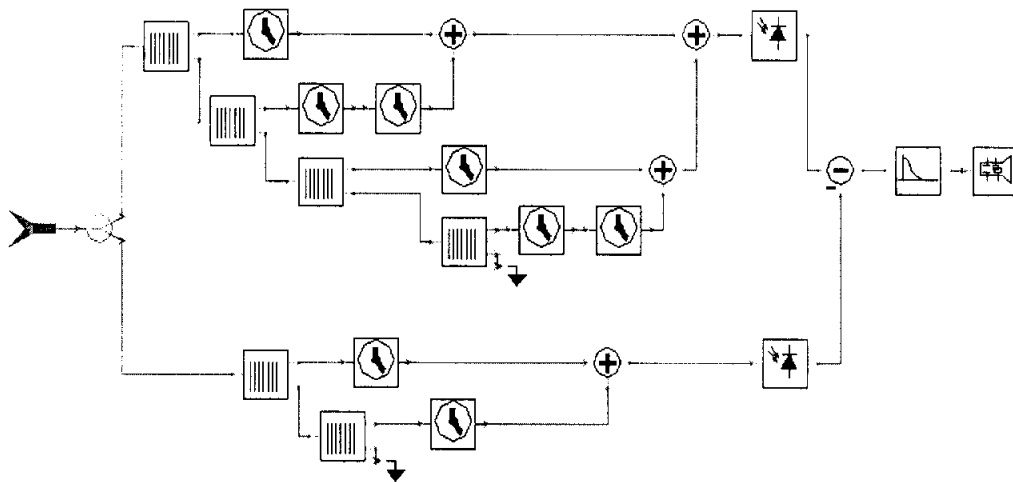


Figure 4.10: Receiver Design for Reduced set of FBGs for Hybrid WDM/SAC system

The received signal in Figure 4.10 is split into two. The upper branch detects pulses with the same spectral distribution $A(v)$ as the intended signal. The lower branch detects one wavelength of each code that correlate with the desired signal. The wavelengths that do not correlate with any other users are chosen using (4.41). Signals that do not correlate with the desired user pass without getting detected.

Figure 4.11 shows the network setup for four users for all the three SAC Optical CDMA systems.

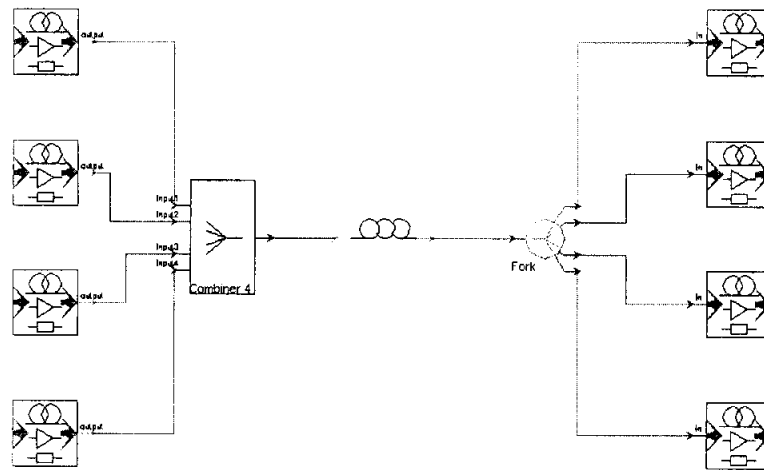


Figure 4.11: Network Setup for four users

All the components used in the simulation are listed in Appendix B.

4.8 Summary

In conclusion, the performance of the DW code family is analyzed using the complementary detection for the basic matrix. A mapping technique is applied to increase the number of users, which changes the cross-correlation of the code sequences to unfixed values, complementary detection is no longer sufficient. A hybrid Wavelength Division Multiplexing/Spectral Amplitude Coding (WDM/SAC) detection scheme is used to solve this problem. A mathematical approach is proposed to reduce the number of Fiber Bragg Gratings (FBG) and minimize the Phase Induced Intensity Noise (PIIN) for

the hybrid WDM/SAC scheme. In addition to improving the performance, this proposed detection scheme can reduce the cost, the processing time and hardware complexity.

A software simulation for a network with four clients is implemented for all the three detection schemes using the Virtual Photonics Instrument (VPI) software version 7.1. Both theoretical and simulation results will be covered in the next chapter.

CHAPTER FIVE

RESULTS AND DISCUSSION

5.1 Introduction

This chapter discusses the results obtained for the DW family code with the systems given in chapter four. This chapter is divided into two main parts; the first part is the theoretical results and the second part is the simulation results obtained by using the Virtual Photonics Instrument (VPI) software.

5.2 Theoretical Results

The performance of the three detection techniques, the complementary detection technique, the hybrid WDM/SAC detection technique and the reduced set of FBGs for WDM/SAC detection technique are evaluated and compared for the DW code family. Theoretical calculation takes into account the Phase Induced Intensity Noise (PIIN), Thermal Noise and Shot Noise, whilst other noises are not taken into consideration.

The parameters used are; Power at the Receiver $P_{sr} = -10 \text{ dBm}$, Operating Wavelength $\lambda_0 = 1550 \text{ nm}$, Center Frequency of the Optical Source bandwidth $\nu_0 = 3.75 \text{ THz}$, Photodetector Quantum Efficiency $\eta = 0.6$, Electrical Bandwidth $B = 1.25 \text{ GHz}$, Data Rate $R_b = 2.5 \text{ Gbps}$, Absolute Receiver Noise Temperature $T_n = 300 \text{ K}$ and Receiver Load Resistance $R_L = 1030 \Omega$.

5.2.1 Comparison between the Complementary and the Hybrid WDM/SAC Methods

Figure 5.1 and Figure 5.2 shows the relation between the Signal to Noise Ratio (SNR) and Bit Error Rate (BER) against the number of simultaneous users respectively, for both complementary SAC and hybrid WDM/SAC systems.

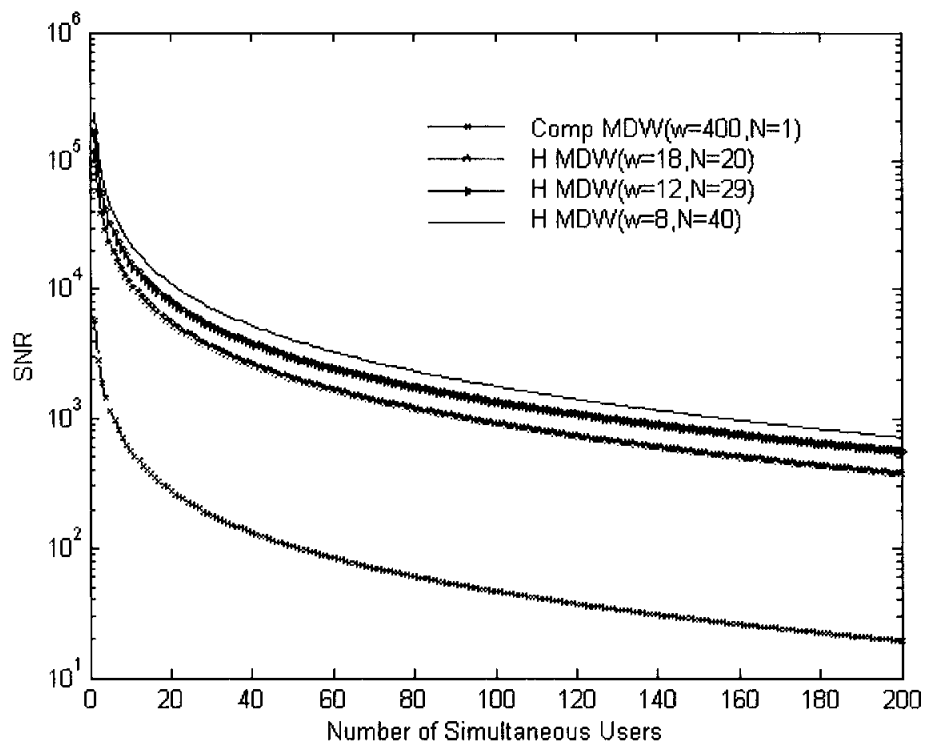


Figure 5.1: SNR versus the number of active users for Complementary and hybrid WDM/SAC

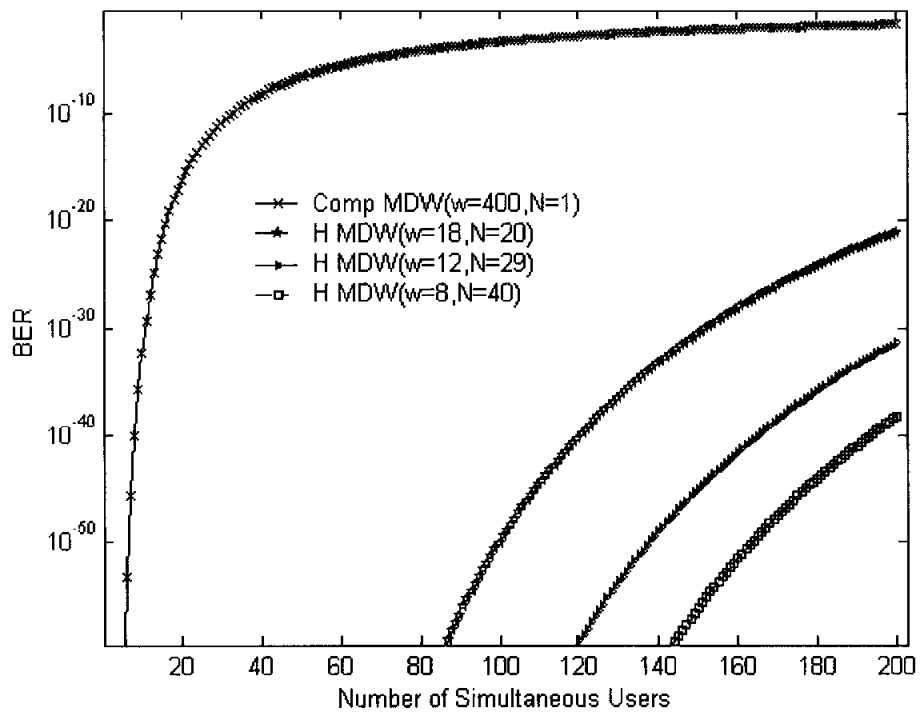


Figure 5.2: BER versus the number of active users for Complementary and hybrid WDM/SAC

Figure 5.1 and Figure 5.2 show the system performance improves when mapping is applied with smaller weights compared to using only the basic number of users (with a large weight) for the same number simultaneous users. This is because when using small weights with mapping the number of overlapping spectra is reduced, leading to a reduction in the PIIN.

5.2.2 Comparison between the Hybrid WDM/SAC and the Reduced FBGs Set Methods

Figure 5.3 shows the variation of the BER to the number of simultaneous users, for both hybrid WDM/SAC and reduced set of FBGs method systems.

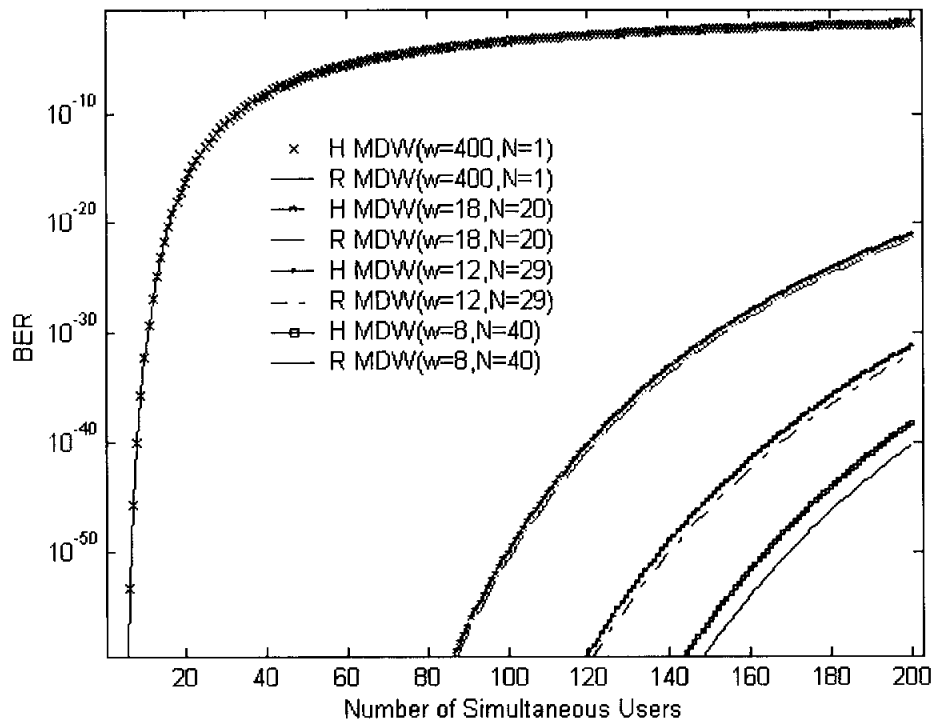


Figure 5.3: BER versus the number of active users for hybrid WDM/SAC and reduced set of FBGs

By applying the proposed reduced method on the hybrid WDM/SAC receiver, better BER is obtained, due to the fact that the PIIN is minimized on the second photodetector. The performance improvement is clearer on smaller weights than on larger weights.

5.3 Simulation Result

The software used is the Virtual Photonics Instruments (VPI) version 7.1. The setup for the simulation is given in chapter four.

5.3.1 Eye Diagram

The Eye diagrams for the complementary detection technique, the hybrid WDM/SAC detection scheme and the Reduced set of FBGs method, for weight four ($w=4$) for both 2.5 Gbps and 10 Gbps and distance of 5 km are investigated.

1. 2.5 Gbps:

Figure 5.4 shows the eye diagram for the complementary SAC system at 2.5 Gbps.

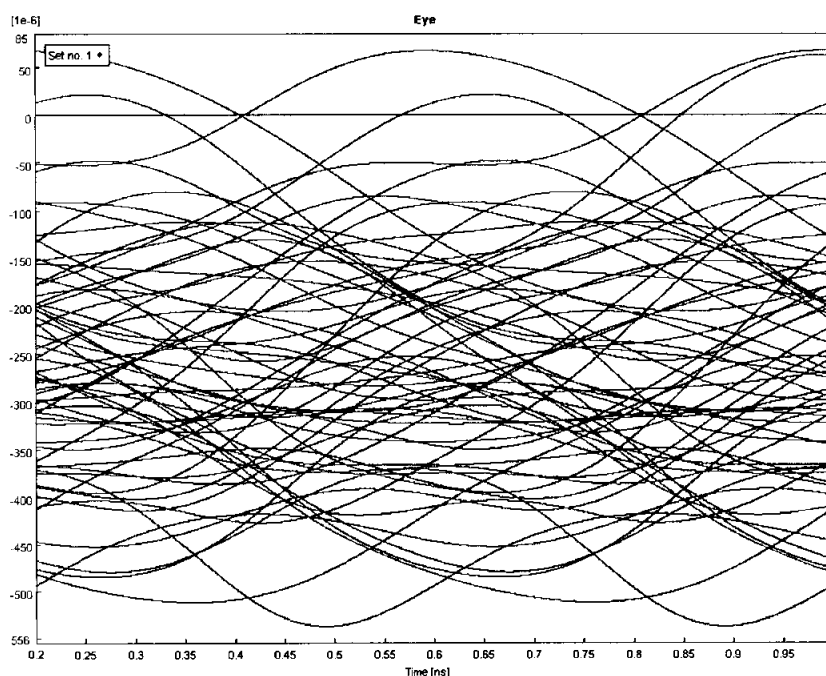


Figure 5.4: Eye Diagram for MDW Code with Complementary SAC at 2.5 Gbps

The eye opening in Figure 5.4 cannot be seen for the complementary detection technique due to the fact that number of users exceeds the basic number (4 rather than 3), balanced detection cannot be achieved because the cross-correlation between all the users is not fixed. The desired signal cannot be retrieved.

Figure 5.5 and Figure 5.6 show the eye diagram for the hybrid WDM/SAC and the reduced set of FBGs at 2.5 Gbps respectively.

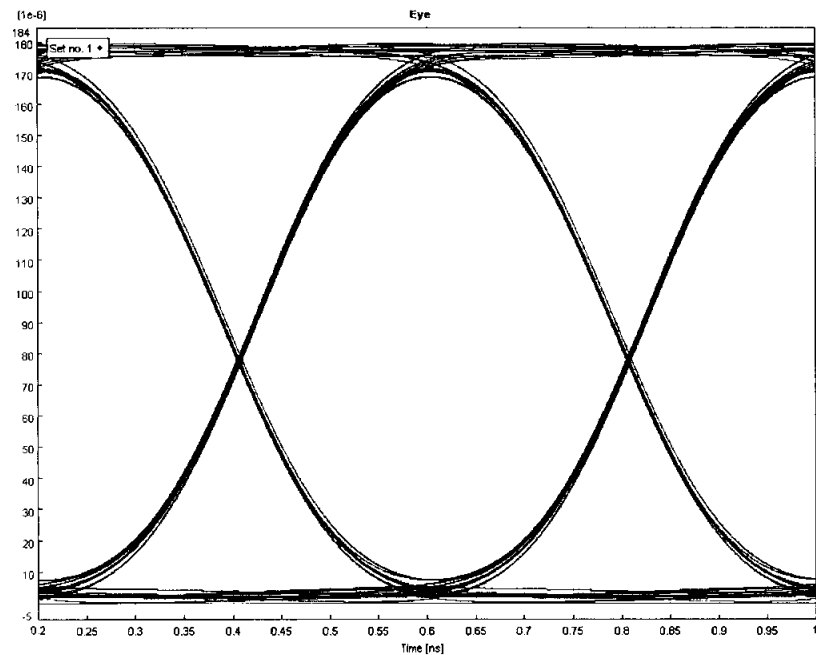


Figure 5.5: Eye Diagram for MDW Code with Hybrid WDM/SAC at 2.5 Gbps

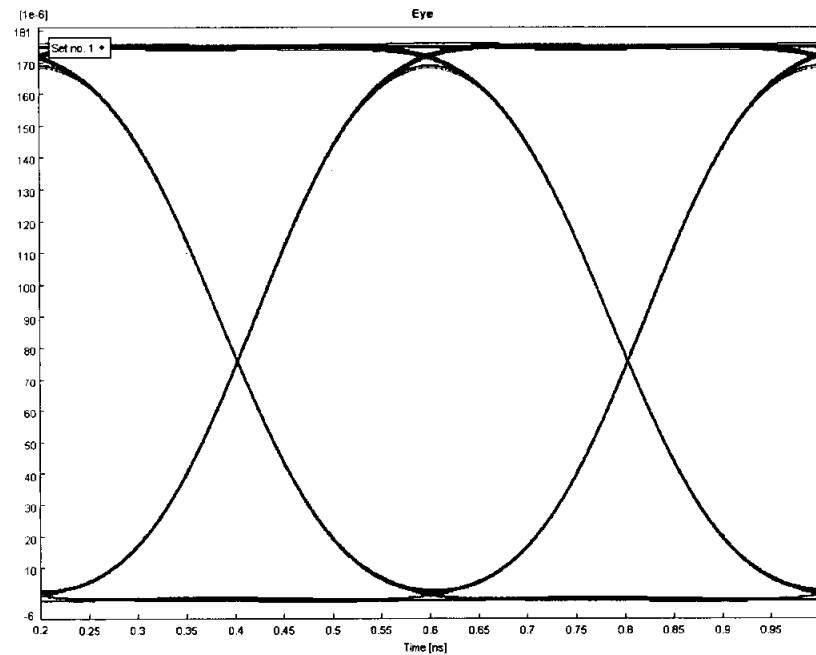


Figure 5.6: Eye Diagram for MDW Code with Reduced set of FBGs for Hybrid WDM/SAC at 2.5 Gbps

It can be observed in Figure 5.5 and Figure 5.6, that both the hybrid WDM/SAC and reduced set of FBGs have a clear eye opening and can detect the intended signal with high precision, because both these techniques support unfixed cross-correlation codes. The reduced set of FBGs shows higher precision than the hybrid WDM/SAC because the PIIN has been minimized at the second photodetector.

2. 10 Gbps:

Figure 5.7 illustrates the same results for complementary detection at a higher data rate, where the eye opening cannot be seen and the intended signal cannot be recovered.

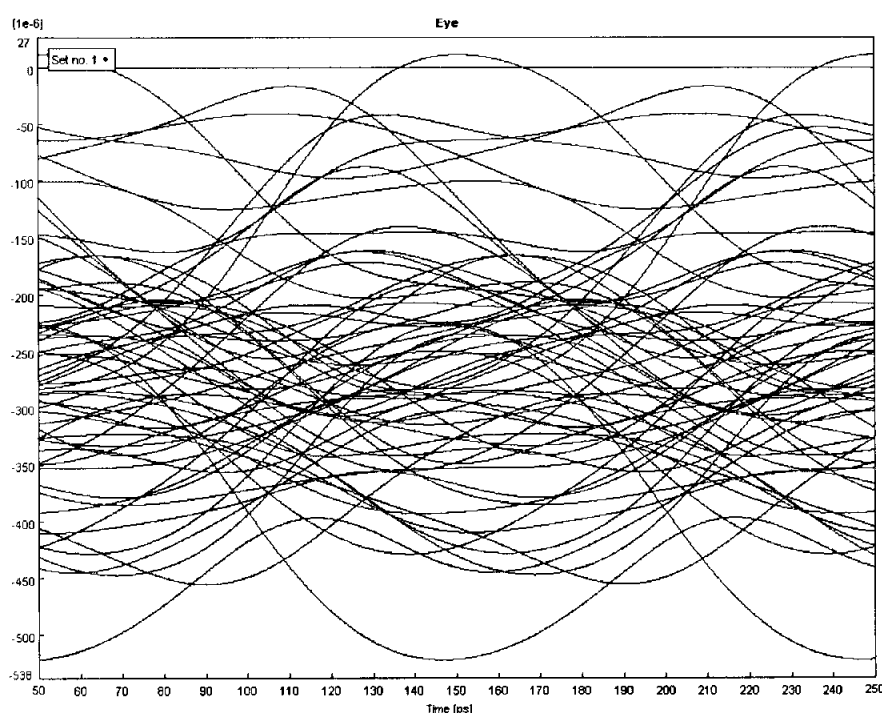


Figure 5.7: Eye Diagram for MDW Code with Complementary SAC at 10 Gbps

Figure 5.8 and Figure 5.9 show the eye diagram for the hybrid WDM/SAC and the reduced set of FBGs at 10 Gbps respectively.

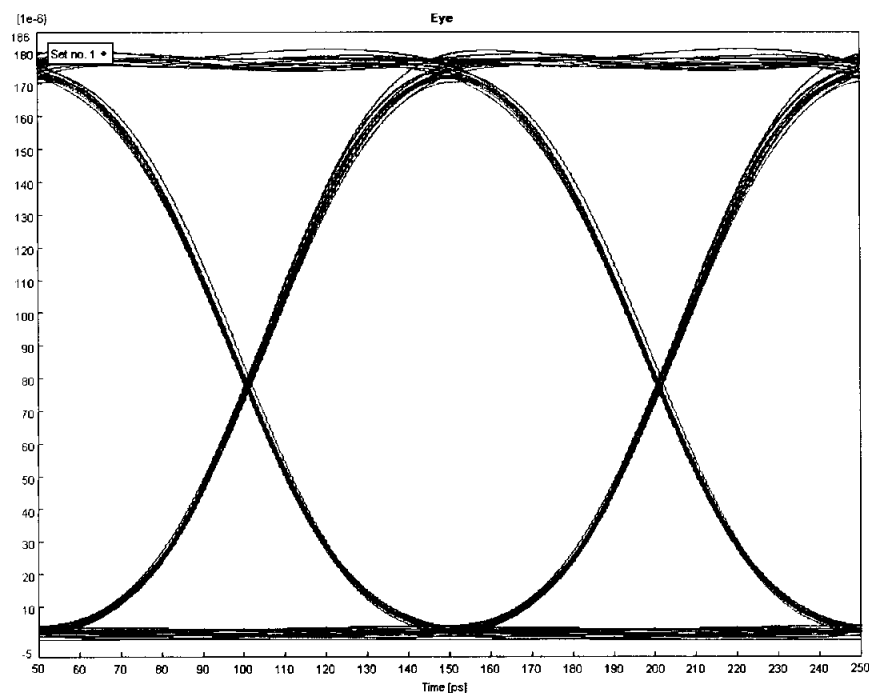


Figure 5.8: Eye Diagram for MDW Code with Hybrid WDM/SAC at 10 Gbps

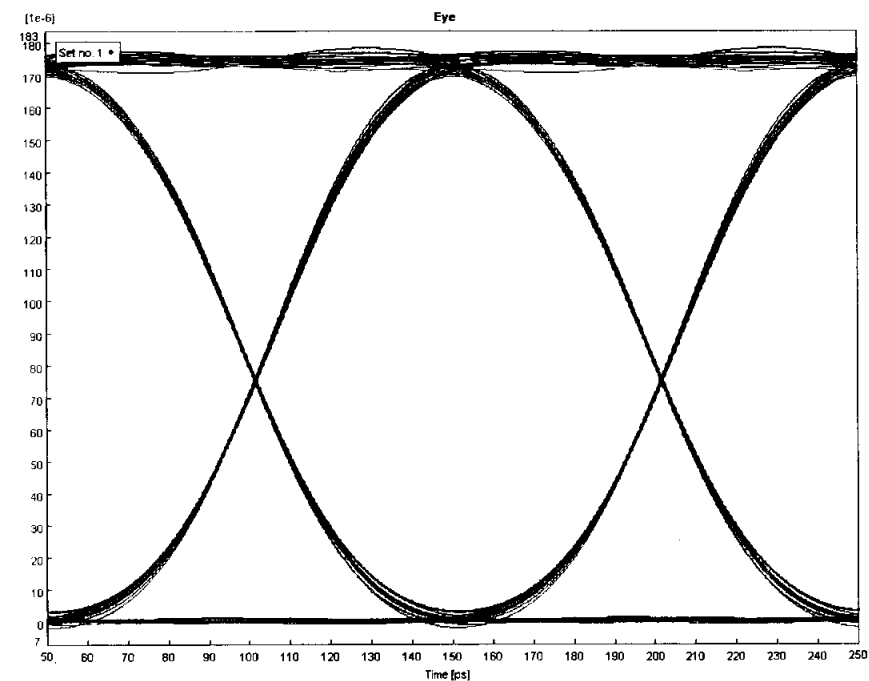


Figure 5.9: Eye Diagram for MDW Code with Reduced set of FBGs for Hybrid WDM/SAC at 10 Gbps

Figure 5.8 and Figure 5.9 show that even at high data rates, both hybrid WDM/SAC and the reduced set of FBGs methods can detect desired signals with minor distortion due to the fibers nonlinearities at high data rates, with some improvement for that latter over the first.

5.3.2 Distance Effect on Bit Error Rate

The Bit Error Rate (BER) is inversely proportional to the distance of transmission, for the fact that longer fibers provide larger attenuation and dispersion which increases the error rate. Figure 5.10 show the BER versus the distance of transmission for both the hybrid WDM/SAC and the reduced set of FBGs.

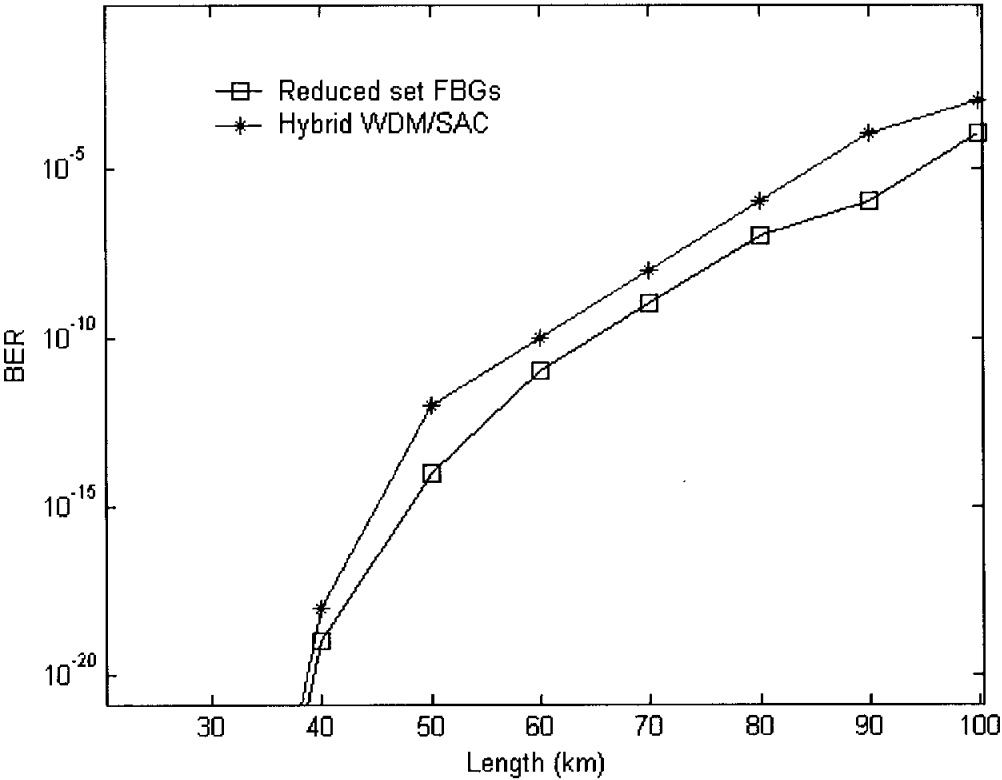


Figure 5.10: BER versus Distance for MDW Code with Hybrid WDM/SAC and reduced set of FBGs at 10 Gbps

Since the reduced set of FBGs has a better performance (less BER) than the hybrid WDM/SAC, for the same transmission quality the reduced set of FBGs can support

longer distances than the hybrid WDM/SAC as shown in Figure 5.10. For example, for a transmission quality of 10^{-12} BER the reduced set method can support a distance up to 55 km, while the hybrid method can support up to 45 km.

5.4 Summary

This chapter discussed the theoretical and simulation results of the detection schemes proposed for the DW family. Results show that by using the hybrid WDM/SAC detection with smaller weights and applying the mapping technique, better BER is achieved than when using the basic number of users with a large weight. Results also show that the proposed reduced set of FBGs method gives better results compared to using only the hybrid WDM/SAC system.

The simulation results show that the complementary method cannot retrieve desired signals when mapping is applied. Results also prove that the proposed reduced FBGs method for MDW code gives better results than the hybrid WDM/SAC system, which enables longer distances of transmission.

CHAPTER SIX

CONCLUSION

6.1 Conclusion

In conclusion, this thesis has investigated the Double Weight (DW) Code Family for Spectral Amplitude Coding (SAC) Optical CDMA systems. The existing code construction for the DW code family, matrix construction and mapping technique have been studied. A new code construction technique has been proposed to overcome the drawbacks of the existing technique which is complicated, insecure and time consuming. Two equation-based techniques have been proposed to construct the DW code family. The first equation is based on the distribution of ones in the code sequences, and the second is based on the distribution of basic building blocks for the basic matrix. Both equations can construct unique codewords without the need to build the whole code sequences for all the users as in the existing technique. These equations are simple, easy to use, efficient and can be applied on any mathematical analysis. A code length equation has also been proposed to calculate the exact code length, which can be used to preset the number of wavelengths needed.

To increase the number of users in the DW code family, a mapping technique is applied. This technique repeats the basic matrix diagonally filling the empty spaces with zeros '0'. Due to this user increment process this cross-correlation property is no longer fixed to one, but it is a mixture of ones for code sequences within the same basic matrix and zeros for sequences which are not in the same basic matrix. The complementary detection technique which is used in SAC Optical CDMA systems cannot be applied because the cross-correlation is no longer fixed to a specific number. A hybrid Wavelength Division Multiplexing/Spectral Amplitude Coding (WDM/SAC) system is used. A mathematical method to reduce the number of Fiber Bragg Gratings (FBG) and minimize the Phase Induced Intensity Noise (PIIN) for the DW code family is proposed. The proposed

method improves the performance and reduces cost, processing time and hardware complexity.

A software simulation with the DW code family is implemented using the Virtual Photonics Instrument (VPI) transmission maker version 7.1. To keep the simulation as real as possible all the different parameters have been included such as, the optical fiber's nonlinearities, shot noise, thermal noise, dark current noise and insertion loss. The study was carried out using various design parameters namely, distance, bit rate and chip spacing. The effect of these parameters on the system was elaborated through the BER, Eye diagrams. Simulation results prove that the reduced set of FBGs for hybrid WDM/SAC gives better results compared to the other detection schemes.

6.2 Future Work

1. Hybrid Systems:

The combinations of Spectral Amplitude Coding with Wavelength Division Multiplexing have a bright future for OCDMA systems, as the two have many advantages.

2. Variable Weight Code Sequences:

As different clients require a different Quality of Service (QoS), a promising area of research is variable weight code sequences.

REFERENCES

- [1] Saleh, B. E. A., Terich, M. C., *Fundamentals of Photonics*, New York: John Wiley & sons, 1991.
- [2] Keiser, G., *Optical Fiber Communication*, Second Edition, New York: McGraw-Hill, 1991.
- [3] Green, P. E. Jr., Englewood Cliffs, N. J., *Fiber Optic Networks*, NJ: Prentice Hall, 1993.
- [4] Dutton Harry J.R., *Understanding Optical Communication*, Prentice Hall ,1998.
- [5] Stamatios V. Kartalopoulos, *Introduction to DWDM Technology Data in rainbow*, WILEY-INTERSCIENCE, 2000.
- [6] Palais, C. Joseph, *Fiber Optic Communications*, Fifth Edition, NJ: Pearson Prentice Hall, 2004.
- [7] Prucnal, P., Santoro, M. Ting Fan, "Spread spectrum fiber-optic local area network using optical processing", *Journal of Lightwave Technology*, May 1986, vol. 4, no. 5, pp. 547- 554.
- [8] Marom, E., Ramer, O.G., "Encoding-decoding optical fiber network", *Electronics Letters*, vol. 14, no. 3, pp. 48-49, 1978.
- [9] Marhic, M.E., "Coherent optical CDMA networks", *Journal of Lightwave Technology*, May 1993, vol. 11, no. 5, pp. 854-864.
- [10] Salehi, J. A., "Emerging Optical Code-Division Multiple Access Communications Systems", *IEEE Network Magazine*, March, 1989, pp. 31-39.
- [11] Karafolas, N., Uttamchandani, D., "Optical Fiber Code Division Multiple Access Networks: A Review", *Optical Fiber technology*, vol. 2, pp. 149-168, 1996.
- [12] Salehi, J. A., "Code division multiple-user techniques in optical fiber networks - Part I", *IEEE Transactions on Communications*, Aug. 1989, vol. 37, no. 8, pp. 824-833.
- [13] Salehi, J. A., Brackett, C. A., "Code division multiple-user techniques in optical fiber networks - Part II", *IEEE Transactions on Communications*, Aug. 1989, vol. 37, no. 8, pp. 834-842.

- [14] Yang, G. -C., Kwong, W. C., *Prime Codes with Application to CDMA Optical and Wireless Networks*, Boston, MA: Artech House 2002.
- [15] Kwong, W. C., Yang, G. -C., "Extended carrier-hopping prime codes for wavelength-time optical code-division multiple-access", *IEEE Transactions on Communications*, July 2004, vol. 52, no. 7, pp. 1084–1091.
- [16] Zaccarin, D., Kavehrad, M., "An optical CDMA system based on spectral encoding of LED," *IEEE Photonics Technology Letters*, Apr. 1993, vol. 4, pp. 479–482.
- [17] Kavehrad, M., Zaccarin, D., "Optical Code-Division-Multiplexed Systems Based on Spectral Encoding of Noncoherent Sources", *Journal of Lightwave Technology*, March 1995, vol. 13, no. 3, pp. 534-545.
- [18] Smith, E. D. J., Blaikie, R. J., and Taylor, D. P., "Performance Enhancement of Spectral-Amplitude-Coding Optical CDMA Using Pulse-Position Modulation", *IEEE Transactions on Communications*, Sept. 1998, vol. 46, no. 9, pp. 1176-1185.
- [19] Zou Wei, H. Ghafouri-Shiraz, "Unipolar Codes With Ideal In-Phase Cross-Correlation for Spectral Amplitude-Coding Optical CDMA Systems", *IEEE Transaction on Communication*, vol. 50, no .8, AUGUST 2002
- [20] Aljunid, S.A., Ismail, M., Ramli, A.R., Borhanuddin M. Ali, Mohamad Khazani Abdullah, "A New Family of Optical Code Sequences for Spectral-Amplitude-Coding Optical CDMA Systems," *IEEE Photonics Technology Letters*, Vol. 16, No. 10, October 2004.
- [21] Wada, N., Kitayama, K. I., "10 Gbit/s Optical Code Division Multiplexing using 8-chip Optical Bipolar Code and Coherent Detection", submitted to *IEEE/OSA Journal of Lightwave Technology Oct 1998*.
- [22] Sardasai, H.P., Chang, C.C, Weiner, A.M., "A Femtosecond code-Division Multiple-Access communication System Test Bed", *IEEE Journal of Lightwave Technology*, November 1998, vol. 16, no. 11, pp. 1953-1964.
- [23] Weiner, A. M., Heritage, J. P., Thurston, R. N., "Synthesis of phase-coherent, picosecond optical square pulses", *Optics Letters*, March, 1986, vol. 11, no. 3, pp. 153-155.
- [24] Weiner, A. M., Heritage, J. P., Salehi, J. A., "Encoding and Decoding of femtosecond pulses", *Optics Letters*, April, 1988, vol. 16, no. 4, pp. 300-302.

- [25] Weiner, A. M., Heritage, J. P., Kirschner, E. M., "High-resolution femtosecond pulse shaping", *Journal of the Optical Society of America B*, Aug. 1988, vol. 5, no. 8, pp. 1563-1572.
- [26] Salehi, J. A., Weiner, A. M., Heritage, Jonathan P., "Coherent Ultrashort Light Pulse Code-Division Multiple Access Communication Systems", *Journal of Lightwave Technology*, Mar. 1990, vol. 8, pp. 478-491.
- [27] Thurston, R. N., Heritage, J. P., Weiner, A. M., Tomlinson, W. J., "Analysis of Picosecond Pulse Shape Synthesis by Spectral Masking in a Grating Pulse compressor", *IEEE Journal of Quantum Electronics*, May 1986, vol. 22, no. 5, pp. 682-696.
- [28] Dinan, E. H., Jabbari, B., "Spreading codes for direct sequence CDMA and wideband CDMA cellular networks", *IEEE Communications Magazine*, Sept. 1998, vol. 36 no. 9 pp. 48-54.
- [29] Komo, J.J., Yuan, C.-C., "Evaluation of code division multiple access systems", *IEEE Proceeding of Energy and Information Technologies in the Southeast*, April 1989, vol. 2, pp. 849-854.
- [30] Yang, G. C., "Performance Analysis for Synchronization and System on CDMA Optical-Fiber Networks", *IEEE Transactions on Communications*, Oct. 1994, no. 10, pp. 1238-1248.
- [31] Kwon, H. M., "Optical Orthogonal Code-Division Multiple-Access System .II. Multibits Sequence-Period", *IEEE Transactions on Communications*, Aug. 1994, vol. 42, no. 8, pp. 2592-2599.
- [32] Chung, F. R., Salehi, J. A., "Optical Orthogonal Codes: Design, Analysis and Applications", *IEEE Transactions on Information Theory*, May 1989, vol. 35, no. 3, pp. 595-604.
- [33] Kostic, Z., Titlebaum, E. L., "The Design And Performance Analysis For Several New Classes Of Codes For Optical", *IEEE Transactions on Communications*, Aug 1994, vol. 42, no. 8, pp. 2608-2617.
- [34] Chung, H., Kumar, P.V., "Optical orthogonal codes-New Bounds and an Optimal Construction", *IEEE Transactions on Information Theory*, July 1990, vol. 36, no. 4, pp. 866-873.

- [35] Yang, G.-C., "Variable-Weight Optical Orthogonal Codes for CDMA Networks with Multiple Performance requirements", *IEEE Transactions on Communications*, January 1996, vol. 44, no. 1, pp. 47-55.
- [36] Yang, G. C and W. C. Kwong, "Performance Analysis of optical CDMA with Prime Codes", *Electronics Letters*, Mar. 1995, vol. 31, No. 7, pp 569-570
- [37] Walle, H., Killat, U., "Combinatorial BER Analysis of Synchronous Optical CDMA with Prime Sequences", *IEEE Transactions on Communications*, Dec. 1995, vol. 43, no. 12, pp. 2894-2895.
- [38] Zhang, J.-G., Kwong, W. C., "Effective design of optical code-division multiple access networks by using the modified prime code", *Electronics Letters*, Jan. 1997, vol. 33, no. 3, pp. 229-230.
- [39] Tancevski, L., Andonovic, I., "Wavelength hopping/time spreading code division multiple access systems", *Electronics Letters*, Aug. 1994, vol. 30, no. 17, pp. 1388–1390.
- [40] Tanceveski, L., Andonovic, I., "Hybrid wavelength Hopping/Time Spreading Schemes for Use in Massive Optical Networks with Increased Security", *IEEE Journal of Lightwave Technology*, vol. 14, no. 12, pp.2636-2647, Dec. 1996.
- [41] Yang, G. C and W. C. Kwong, "Performance Comparsaon of Multiwavelength CDMA and WDMA + CDMA for Fiber-Optic Networks", *IEEE Transactions On Communications*, Nov. 1997 , vol. 45, no. 11, pp. 1426-1434
- [42] Yang, G. C. and Kwong, W. C., "Performance analysis of extended carrier-hopping prime codes for optical CDMA". *IEEE Transactions on Communications*, May 2005, vol. 53, no. 5, pp. 876– 881.
- [43] D. Zaccarin and M. Kavehrad, "New architecture for incoherent optical CDMA to achieve bipolar capacity," *Electronics Letters*, Feb. 1994, vol. 30, no. 3, pp. 258–259.
- [44] D. Zaccarin and M. Kavehrad, "Optical CDMA with new coding strategies and new architectures to achieve bipolar capacity with unipolar codes," in *OFC'94 Technology Dig.*, 1994, pp. 168–170.
- [45] Zhou, X., Shalaby, H. M. H., Lu, C., "Design and performance analysis of a new code for spectral-amplitude-coding optical CDMA systems," in *IEEE 6th Int. Symp. Spread Spectrum Techniques Applications*, Spet. 2000, vol. 1, pp. 174–178.

- [46] Wei, Z., Shalaby, H. M. H., Ghafouri-Shiraz, H., “Modified quadratic congruence codes for fiber Bragg-grating-based spectral-amplitude coding optical CDMA systems”, *Journal of Lightwave Technology*, Sept. 2001, vol. 19, no. 9, pp. 1274-1281.
- [47] Zou Wei, Ghafouri-Shiraz, H., “Codes for Spectral-Amplitude-Coding Optical CDMA Systems”, *Journal of Lightwave Technology*, Aug. 2002, vol. 50, no. 8, pp. 1209-1212.
- [48] Syed Alwee Aljunid, Zuraidah Zan, Siti Barirah Ahmad Anas and Mohd. Khazani Abdullah “A New Code for Optical Code Division Multiple Access Systems”, *Malaysian Journal of Computer Science*, Dec. 2004, vol. 17, no. 2, pp. 30-39.
- [49] Moslehi, B., “Noise power spectra of optical two-beam interferometers induced by the laser phase noise”, *Journal of Lightwave Technology*, Nov. 1986, vol. 4, no. 11, pp. 1704–1710.
- [50] Prucnal, Paul R., *Optical Code Division Multiple Access: Fundamentals and Applications*, Taylor and Francis Group, 2005.
- [51] Lachs, Gerard, *Fiber Optic Communications Systems, Analysis and Enhancement*, McGraw Hill Telecommunications, 1998.
- [52] Chao-Chin Yang “Hybrid Wavelength-Division Multiplexing/Spectral-Amplitude-Coding Optical CDMA System”, *IEEE Photonics Technology Letters*, June 2005, vol. 17, no. 6, pp. 1343 – 1345.

PUBLICATIONS

- [1] **A. Mohammed**, E.I. Babekir, N. Elfadel, N.M. Saad, M.S. Anuar, S.A. Aljunid, M.K. Abdullah, "New Approach of Double Weight Code Family Detection Using Reduced Set of Fiber Bragg Gratings", *IEEE International Conference on Wireless and Optical Communications Networks (WOCN 2007)*, 2nd-4th July 2007, Singapore, Republic of Singapore.
- [2] **A. Mohammed**, E.I. Babekir, N. Elfadel, N.M. Saad, M.S. Anuar, S.A. Aljunid, M.K. Abdullah, "OSCDMA Double Weight Code: A Simplified Formula Code Construction Technique", *IEEE International Conference on Wireless and Optical Communications Networks (WOCN 2007)*, 2nd-4th July 2007, Singapore, Republic of Singapore.
- [3] **A. Mohammed**, N.M. Saad, E.I. Babekir, N. Elfadel, S.A. Aljunid, M.S. Anuar, M.K. Abdullah "OSCDMA Double Weight Code: Analysis On The Detection Scheme For The Mapping Technique", *IEEE International Conference on Telecommunications and Malaysia International Conference on Communication (ICT-MICC 2007)*, 14th-17th May 2007, Penang, Malaysia.
- [4] **A. Mohammed**, N.M. Saad, S.A. Aljunid, A.M. Safar, M.K. Abdullah "Optical Spectrum CDMA: A New Code Construction for Double Weight Code Family", *IEEE International Symposium on Communications and Information Technologies (ISCIT 2006)*, 18th-20th Oct. 2006, Bangkok, Thailand.
- [5] **A. Mohammed**, N.M. Saad, "Optical Spectrum CDMA Double Weight Code Family using Equation-Based Code Construction", *MMU International Symposium on Information and Communications Technologies (M²USIC 2006)*, 16th-17th Nov. 2006, Kuala Lumpur, Malaysia.

APPENDIX A

Optical Codes:

TABLE I
CODEWORDS SET OF AN OPTIMAL OOC(341, 5, 1) CODE

| | | | | | |
|----------|---|----|-----|-----|-----|
| S_1 | 0 | 1 | 85 | 21 | 5 |
| S_2 | 0 | 2 | 170 | 10 | 42 |
| S_3 | 0 | 3 | 111 | 104 | 53 |
| S_4 | 0 | 6 | 222 | 106 | 53 |
| S_5 | 0 | 9 | 268 | 151 | 105 |
| S_6 | 0 | 11 | 45 | 76 | 198 |
| S_7 | 0 | 12 | 103 | 75 | 212 |
| S_8 | 0 | 13 | 305 | 227 | 43 |
| S_9 | 0 | 15 | 107 | 146 | 164 |
| S_{10} | 0 | 17 | 264 | 203 | 165 |
| S_{11} | 0 | 19 | 88 | 267 | 220 |
| S_{12} | 0 | 22 | 90 | 55 | 152 |
| S_{13} | 0 | 23 | 293 | 252 | 118 |
| S_{14} | 0 | 24 | 206 | 83 | 150 |
| S_{15} | 0 | 25 | 54 | 169 | 221 |
| S_{16} | 0 | 26 | 269 | 86 | 113 |
| S_{17} | 0 | 37 | 147 | 217 | 81 |

TABLE II
PRIME CODE OVER $GF(5)$

| | |
|-----|-------------------------------|
| i | C_i |
| 0 | 10000 10000 10000 10000 10000 |
| 1 | 10000 01000 00100 00010 00001 |
| 2 | 10000 00100 00001 01000 00010 |
| 3 | 10000 00010 01000 00001 00100 |
| 4 | 10000 00001 00010 00100 01000 |

TABLE III
EXAMPLE OF THE (8 x 41, 8, 0, 1) CARRIER-HOPPING PRIME CODE. THE FOUR
MATRICES REPRESENT THE CODE SEQUENCES X₄, X₉, X₁₁, AND X₂₂,
RESPECTIVELY.

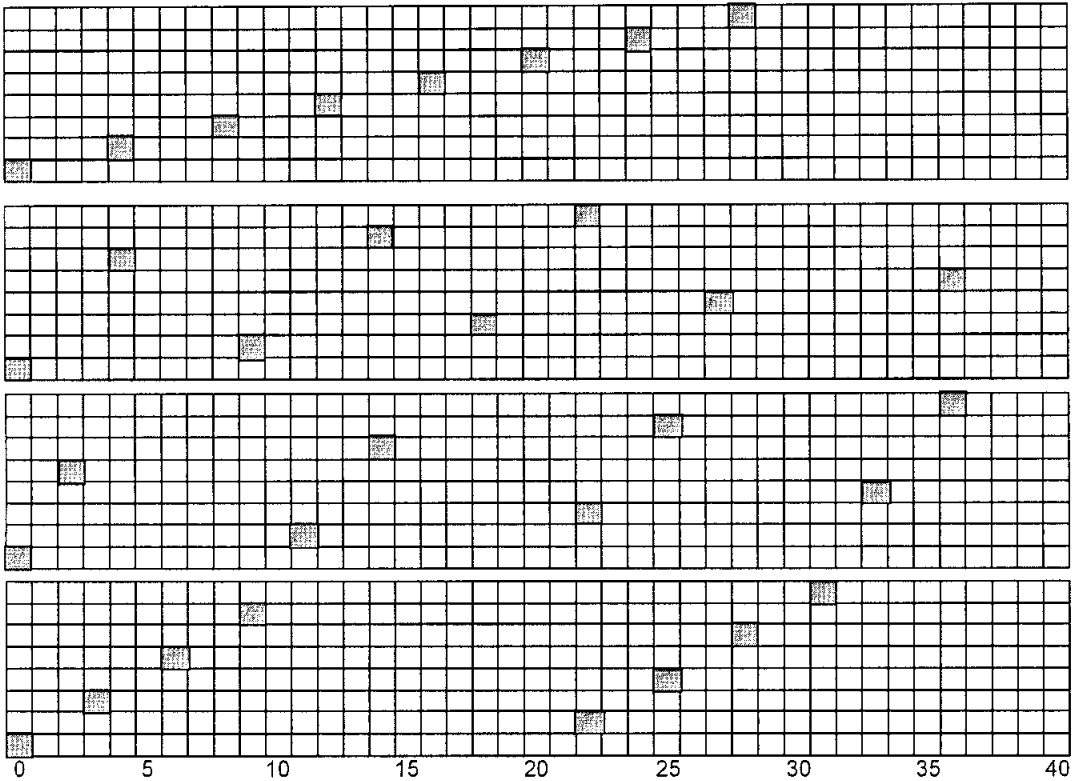


TABLE IV
EXAMPLE OF BIBD CODE (q=2; m=2 IRREDUCIBLE POLYNOMIAL OF GF(8):
X³+X+1)

| <i>y(k)</i> | <i>s(i)</i> |
|-------------|-------------|
| (1 2 4) | 1101000 |
| (2 3 5) | 0110100 |
| (3 4 6) | 0011010 |
| (4 5 7) | 0001101 |

TABLE V
EXAMPLE OF MQC CODE

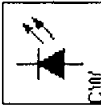
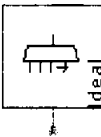
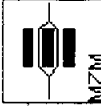
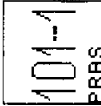


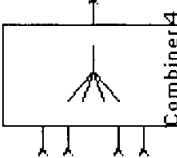
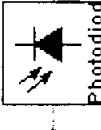
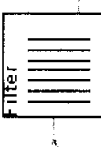

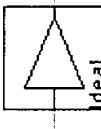
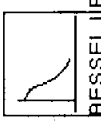
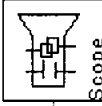
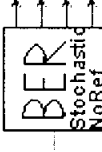
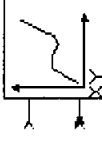

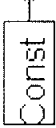

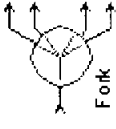
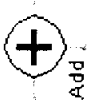




| | $y(k)$ | $s(i)$ |
|---------------------|-----------------|-------------------------------------|
| $\alpha=0, \beta=0$ | (0 1 4 4 1 2) | 10000 01000 00001 00001 01000 00100 |
| $\alpha=1, \beta=0$ | (1 4 4 1 0 3) | 01000 00001 00001 01000 10000 00010 |
| $\alpha=4, \beta=0$ | (1 0 1 4 4 1) | 01000 10000 01000 00001 00001 01000 |
| $\alpha=1, \beta=3$ | (4 2 2 4 3 3) | 00001 00100 00100 00001 00010 00010 |
| $\alpha=3, \beta=4$ | (3 0 4 0 3 0) | 00010 10000 00001 10000 00010 10000 |

TABLE VI
EXAMPLE OF MFH CODE

| | $y(k)$ | $s(i)$ |
|--------------------------|---------------|--------------------------|
| $\alpha=0, b=0$ | (1 2 3 0 0) | 0100 0010 0001 1000 1000 |
| $\alpha=1, b=0$ | (2 3 1 0 1) | 0010 0001 0100 1000 0100 |
| $\alpha=2, b=1$ | (2 0 3 1 2) | 0010 1000 0001 0100 0010 |
| $\alpha=0, b=3$ | (2 1 0 3 0) | 0010 0100 1000 0001 1000 |
| $\alpha=2, b=2$ | (1 3 0 2 2) | 0100 0001 1000 0010 0010 |
| $b=1 \text{ for } y'(k)$ | (1 1 1 1 3) | 0100 0100 0100 0100 0001 |

APPENDIX B

List of components used in the simulation

| | | | | | |
|---|---|---|---|---|---|
|  |  |  |  |  |  |
| Laser CW_vtms1 | WDM_MUX_N_1_Ideal_vtms1 | Modulator M2_vtms1 | PRBS_vtms1 | Coder NRZ_EI_vtms1 | Rise TimeAdj_vtms1 |
|  |  |  |  |  |  |
| Combiner4 Combiner_4_1_vtmg1 | Photodiode_vtms1 | FilterFBG_vtms1 | Fiber NLS_vtms1 | Ideal | FilterBesselLP_EI_vtms1 |
|  |  |  |  |  |  |
| VScope_vtms1 | BER_Stochastic_NoRef_vtms1 | VMXY_vtms1 | ClockRecovery/Ideal_vtms1 | Const_vtms1 | Fork |
|  |  |  |  |  |  |
| Fork | Add | - | output_vtmy1 | input_vtmy1 | Fork |